Legacies of past human activities on one of the largest old-growth forests in the south-east European mountains

Eleonora Cagliero, Donato Morresi, Laure Paradis, Milic Curovic, Velibor Spalevic, Niccolò Marchi, Fabio Meloni, Ilham Bentaleb, Renzo Motta, Matteo Garbarino, et al.

Legacies of past human activities on one of the largest old-growth forests in south-east European mountains

Eleonora Cagliero[1,2], Donato Morresi[3], Laure Paradis[2], Milić Čurović[4], Velibor Spalevic[5], Niccolò Marchi[1], Fabio Meloni[3], Ilham Bentaleb[2], Renzo Motta[3], Matteo Garbarino[3], Emanuele Lingua[1], Walter Finsinger[2]

[1] Department of Land, Environment, Agriculture and Forestry (TESAF), University of Padova, 35020 Legnaro (PD), Italy

[2] University of Montpellier, ISEM, CNRS, IRD, EPHE, Montpellier, France

[3] Department of Agricultural, Forest and Food Sciences (DISAFA), University of Torino, 10095 Grugliasco (TO), Italy

[4] University of Montenegro, Biotechnical Faculty, Podgorica, Montenegro

[5] University of Montenegro, Faculty of Philosophy – Geography Department, Nikšić, Montenegro

Walter Finsinger

Institut des Sciences de l'Evolution-Montpellier (ISEM)
CNRS – EPHE - IRD
Montpellier
France

Correspondence and requests should be addressed to:
walter.finsinger@umontpellier.fr, +33 (0)6 69 61 07 42

Abstract

The Dinaric Mountains are a region considered as a hotspot for remaining late-successional montane mixed *Abies alba-Fagus sylvatica-Picea abies* old-growth forests presumably because historical deforestation levels were substantially lower than in other European regions. We present new well-dated stand-scale palaeoecological records (pollen, spores, stomata, macrofossils, macroscopic charcoal, and magnetic susceptibility), an extensive dataset of current forest structures and a detailed land-cover types map from the Biogradska Gora forest to provide new insights into the long-term vegetation dynamics of old-growth forests in the montane zone of the Dinaric Mountains. Land use (cereal crop cultivation, cattle herding, and fire) during the Middle Ages caused a reduction of the *A. alba* and *P. abies*-dominated forest. After a major land-abandonment event around the Black Death pandemic (mid-14th century) and more moderate land-use phases associated with fire episodes, which favoured the short-term expansion of light-demanding pioneer species (*Corylus* and *Betula*), *F. sylvatica*-dominated stands developed in the more accessible outer part of the forest. The legacy of past land uses is still visible as the structure of the almost pure *F. sylvatica* stands shows less old-growth characteristics. Most strikingly and markedly in contrast to decreasing tree cover due to generally intensifying land use elsewhere in Europe, tree cover increased several centuries before the formal protection of the forest (1878 CE), supporting the view that historical land-use pressures played an important role for the small extent and the continuity of disturbance-sensitive *A. alba* and *P. abies*-dominated old-growth stands.

Keywords

disturbance history; forest structure; land-use legacy; mountain ecosystem; old-growth forest; palaeoecology

Introduction

Forest ecosystems that have developed for a long period of time without important anthropogenic disturbance are rare (<3% of the total forest extent), small and fragmented in Europe (Sabatini et al. 2018; Barredo et al. 2021). Major human imprints on many, if not all, forest ecosystems, including high conversion rates to agriculture (often with the use of fire) for millennia and intense forest exploitation (Kaplan et al. 2009; Birks and Tinner 2016) are generally viewed as causes for their current small extent (Nagel et al. 2017; Sabatini et al. 2020). Despite their small extent, these primary and old-growth forests provide valuable opportunities to study forest dynamics and biotic responses to non-anthropogenic disturbances (Foster et al. 1996), thereby contributing to the development of close-to-nature forest management methods (Bauhus et al. 2009; Schütz et al. 2016) and guiding restoration and adaptation to environmental changes (Mazziotta et al. 2016). Even if generally protected and particularly the smaller ones (<1000 ha), these forests are vulnerable to both biotic and abiotic disturbances (Nagel et al. 2017; Sabatini et al. 2020), climate change (Elsen et al. 2020) as well as by land-use and altered disturbance regimes (e.g. fires) in surrounding areas (Hansen and DeFries 2007) that may hinder the development of features associated with old-growth stage.

Old-growth forests are typically characterised by functional, structural and compositional features which distinguishes them from forests of younger age classes: high amounts and size of deadwood, presence of old trees approaching their natural longevity and a mosaic of heterogeneous stands arising through gap dynamics (Wirth et al. 2009). These features indirectly reflect the length of time an area has been continuously wooded without human influence and major stand-replacing disturbances, as well as the history of land-use and forest management (Buchwald 2005). However, features reflecting the old-growthness of current forest structures cannot provide information on their longer-term history and dynamics. Paleoecology, instead, is sometimes the best and only tool for evaluating the history and ecosystem responses to past environmental changes such as climate, fire and land use (Whitlock et al. 2018). Moreover, palaeoecology can document the legacies of land-use history, climate change and disturbances such as fire on present-day forest composition (Lindbladh 1999; McLachlan et al. 2000; Birks 2019), which is a critical information for clarifying conservation objectives and evaluating outcomes (Whitlock et al. 2018; McMullin and Wiersma 2019).

The distribution of primary and old-growth forests is uneven in Europe, likely because the intensity and extent of human pressure differed among regions (Sabatini et al. 2020). Old-growth forests in east-central Europe have captured the attention of foresters long ago (Leibundgut 1959; Horvat et al. 1974) as their dominant tree species (*Abies alba* Mill., *Fagus sylvatica* L., and *Picea abies* (L.) Karst) prevail in the montane belt of central Europe.

For instance, the Dinaric Mountains is considered a hotspot for late-successional montane old-growth forests (Sabatini et al. 2018) presumably due to early protection of forests during the 19th century and lower historical human pressure compared to other mountain ranges in Europe due to the extent of rugged mountain areas and land with low agricultural productivity (Diaci 1999; Kaplan et al. 2009; Nagel et al. 2017). However, records documenting long-term vegetation dynamics in conjunction with environmental changes are lacking for the montane zone in this region (Finsinger et al. 2017). Thus, the factors leading to their fragmentation and the extent to which the current landscape retains legacies of past land-uses and natural components (Vale 2002; Whitlock et al. 2018) are largely unknown. For instance, in the montane zone of the Apennines, monospecific beech forests established in relatively recent times following the decline of *Abies alba* and other mesophilous deciduous trees due to enhanced fire activity and multi-millennial land-use intensification superimposed on late-Holocene cooling and moistening (Morales-Molino et al. 2020).

Here, we present novel multi-proxy palaeoecological data (pollen, spores, macrofossils, macroscopic charcoal, and magnetic susceptibility) and current forest structure data from Biogradska Gora (central Dinaric Mountains, Montenegro) to provide new insights into the long-term vegetation dynamics of old-growth forests in the montane zone of the Dinaric Mountains. The forest has been continually under protection for the past 140 years and includes one of the largest central-southern European old-growth stands dominated by mixed fir and beech with sparse spruce that is surrounded by almost pure beech stands (Motta et al. 2015a). Our specific aims are: (1) to assess differences in current forest structure within the old-growth stands and the surrounding forest, (2) to track stand-scale long-term vegetation dynamics and occurrence of past disturbances by fire, and (3) assess potential legacy effects on present-day forests.

Materials and Methods

Study area

The Biogradska Gora valley (Fig. 1) is located on the Bjelasica massif, which bears relatively small amounts of carbonate bedrocks compared to the rest of the Dinaric mountain system, where limestone substrata are prevalent. Dystric cambisols (brown soils) on eruptive rock are the dominant type of soil (Čurović et al. 2011). The climate is influenced by continental and maritime airstreams, with annual average precipitation of *c*. 1960 mm, lowest rainfall in July-August and monthly temperatures ranging between -2 and 16 ºC (Motta et al. 2015a; Fick and Hijmans 2017).

Tree cover in the valley is dominated by beech, fir and spruce, with minor amounts of *Acer pseudoplatanus* L., *A. platanoides* L. and *A. heldreichii* Orph. ex Boiss, *Fraxinus excelsior* L., *Ulmus montana* With., *Ulmus glabra* Huds., and *Sorbus aucuparia* L. (Stijovic 2017). *Betula* L. and *Pinus mugo* Turra occur at the upper treeline in adjacent valleys, and *Pinus peuce* Griseb*, P. leucodermis* Ant.*,* and *P. sylvestris* L. are absent in the valley but sparsely occur on the Bjelasica (Černjavski 1937).

The forest is protected since 1878 CE, when the area was set aside as a royal hunting reserve (Motta et al. 2015a). The area is included in the Biogradska Gora National Park since 1952 to protect the forest from exploitation by logging companies (Luburić 2016) and has been proclaimed Biosphere Reserve in 1977 (UNESCO 2010). This includes a 2830-ha strictly protected core area (IUCN category II) where land-use activities (logging, farming, grazing) are prohibited. The core area is surrounded by a buffer zone characterised by meadows (Fig. 1) and groups of shepherds' huts (locally called "*katun*") whose presence possibly dates back to the Middle Ages when pasturing was widespread in Montenegro (Pluskowski and Seetah 2006). The number of occupied huts has declined considerably during the past decades due to rural areas depopulation and many of them have been converted for tourism purposes.

Current forest composition and structure

We surveyed 51 plots predominantly in the outer part of the forest (Fig. 1). Their location was guided by a preliminary segmentation of a SPOT5 satellite image that identified polygons of homogeneous forest canopy composition and structure (Motta et al. 2015a).

In each circular plot (radius = 14 m), we recorded the species and measured the diameter at breast height (DBH) of all living stems with a DBH ≥ 7.5 cm and the heights (H) of at least three individuals for each species and in different diameter classes when available. We measured the minimum and maximum diameter and length (D_{min}, D_{max}, L) of all coarse woody debris (CWD) with L ≥ 100 cm and D_{min} ≥ 10 cm, classifying the deadwood as snags (standing dead trees), logs (lying deadwood), or stumps (H<130 cm). In a smaller area (radius = 6 m) centred on each plot centroid we identified and counted the regeneration (DBH < 7.5 cm).

We pooled our 51-plots dataset with the 30-plots dataset recorded by Motta et al. (2015), which were concentrated in a small (50 ha) portion of the inner part of the forest, and for each plot calculated variables to assess the current old-growthness and forest structure. Then we estimated the overall tree density (De; #/ha), basal area (BA; m^2/ha), and amount of regeneration (Re; #/ha). To estimate the volume of living wood biomass (V; m^3/ha) we used a local volume table, deriving tree heights from species-specific hypsometric curves. We computed CWD volumes

144 (m^3/ha) for CWD classes, and the dead to live wood ratio (Öder et al. 2021). To estimate tree species diversity, we
145 computed the Brillouin index (Brillouin 1956). To measure the structural diversity, we calculated the DBH
146 standard deviation, Tree Diameter Diversity index (TDD) to 5 cm DBH classes of living stems (Rouvinen and
147 Kuuluvainen 2005), and the Gini coefficient (Gini 1912; Weiner and Solbrig 1984), which quantifies the structural
148 heterogeneity in tree diameters (G_{DBH}) and basal areas (G_{BA}) (Table S1).
149 Subsequently, we identified forest structural types (FST) using a Hierarchical Cluster Analysis (HCA) based on
150 selected structural and compositional variables and tested the statistical differences among FSTs using a non-
151 parametric Kruskal-Wallis test, followed, in the case of significance, by a Dunn's post hoc test (see ESI1 for further
152 details).
153 To explore the influence of accessibility, we calculated Spearman's correlations between variables describing
154 forest structure and a proxy for potential human pressure namely the cost of access, that is the minimum
155 accumulative distance (m) to each plot from the main roads (see ESI1 for further details), following Garbarino et
156 al. (2013).
157 To assess the distribution of land-cover types and to upscale FSTs at a landscape scale we used an object-based
158 image analysis. We pre-processed two high-resolution satellite images (Table S2) by pan-sharpening multispectral
159 bands through the nearest neighbour diffusion (NNDiffuse) algorithm (Sun et al. 2014) and by co-registering them
160 to the Bing satellite image with ENVI software (v5.3.1; Exelis Visual Information Solutions, Boulder, Colorado).
161 We then created image objects through the Large-Scale Mean-Shift (LSMS) segmentation algorithm (Michel et
162 al. 2015) implemented in Orfeo ToolBox v7.0 (Grizonnet et al. 2017), using a raster stack formed by the near
163 infrared band, the Normalized Difference Vegetation Index (NDVI) and textural data derived from granulometric
164 analysis based on the opening procedure (see ESI1 for further details). We performed a supervised classification
165 of image objects using the Random Forest (RF) algorithm implemented in the 'ranger' R package (Wright and
166 Ziegler 2017), employing the spectral and textural information of the image objects as predictor variables for the
167 RF model (Table S3). We trained the RF model using 1457 objects that were classified through on-screen visual
168 interpretation. Most of the training objects (n=1305) intersected the 81 ground-survey plots and belonged to one
169 of the following land-cover types: broadleaved trees, conifers and forest canopy gaps. We identified training
170 objects of land-cover types that we did not survey (grasslands, bare ground and water) through on-screen
171 interpretation. We assessed the performance of the RF model by computing the average overall accuracy and
172 Cohen's Kappa statistic obtained from a 5-fold cross-validation procedure. We performed the analyses separately
173 for two satellite images and then merged the land-cover maps.

174

175 ***Long-term vegetation and fire disturbance histories***

176 We collected a 245-cm long sediment sequence from a small pond (0.047 ha; 42°54'5.898"N; 19°35'53.538"E;
177 1155 m a.s.l.; Fig. 1) located in the beech-dominated outer part of the forest to reconstruct stand-scale vegetation
178 dynamics. We combined two parallel and overlapping cores (drives 1-m long and 8 cm in diameter) collected near
179 to the centre of the basin with a Russian-type corer at 5 cm water depth.

180 To constrain the depth-age model, we used eight AMS ^{14}C dates from terrestrial plant macrofossils (Table S4)
181 calibrated using the IntCal13 dataset (Reimer et al. 2013). We built the model using the RBacon v2.4.1 package
182 (Blaauw and Christen 2011) and verified the accuracy in its most recent part by comparing the expected and actual
183 ages of the first occurrence of *Ambrosia artemisiifolia* L. pollen. Documentary evidence (Makra et al. 2005;
184 Csontos et al. 2010) indicates that ragweed (*Ambrosia*) became invasive in Central and Eastern Europe around
185 1910-1920 CE.

186 We measured the magnetic susceptibility at 1-cm intervals with a Bartington MS2E surface-scanning sensor
187 following Nowaczyk (2001). Magnetic susceptibility is influenced by the amount of minerogenic input that results
188 from erosion. Negative magnetic-susceptibility values are found in sediments with minerals that do not contain Fe
189 (e.g. quartz and calcite) and in organic-rich sediments.

190 We used macroscopic charcoal analyses to reconstruct long-term fire activity (Whitlock and Larsen 2001;
191 Conedera et al. 2009). We counted charcoal particles in contiguous 1-cm^3 samples, and additionally measured
192 areas of charcoal particles for 42 samples (6-cm resolution) using an image-analysis software (see ESI1). We
193 transformed charcoal concentrations to charcoal accumulation rates (CHAR) based on the chronology.

194 To uncover local-scale vegetation dynamics, we analysed 41 plant macrofossil samples in conjunction with pollen
195 and stomata (see Fig. S1 and ESI for details of laboratory and identification methods used) (Birks and Birks 2000;
196 Ammann et al. 2014; Finsinger and Tinner 2020). We calculated pollen percentages relative to the terrestrial pollen
197 sum, which included pollen from trees, shrubs, herbs and *Pteridium* spores. A sum of at least 250 pollen and spores
198 was counted for each sample. However, the lowermost sample has a substantially lower pollen sum (n=36) due to
199 an extremely low pollen concentration.

200 To evaluate human impact, we considered the abundances of primary anthropogenic indicators, secondary
201 adventives and apophytes (Behre 1981; Deza-Araujo et al. 2020), which include pollen of cultivated plants,
202 ruderals, and plants of meadows. In addition, we used *Sporormiella*-type dung-fungi spores, which are linked to
203 the presence and abundance of large herbivores (Davis 1987; Baker et al. 2013), and *Tilletia caries*-type spores

(see ESI1), a pathogen associated mostly with grasses, including cereals (Mazurkiewicz-Zapałowicz and Okuniewska-Nowaczyk 2015). Abundances of non-pollen palynomorphs are presented as influx (number cm^{-2} $year^{-1}$).

We determined pollen assemblage zones based on terrestrial pollen taxa (excluding taxa with maximum abundance <5%) using optimal partitioning by sums-of-squares (Birks and Gordon 1985) in Psimpoll v4.26 (Bennett 2008). The number of statistically significant zone boundaries was determined by comparison with the broken-stick model (Bennett 1996).

We analysed the CHAR data using CharAnalysis v1.1 (Higuera et al. 2009) to determine centennial-scale trends in CHAR that were interpreted as relative changes in biomass burned over time (Marlon et al. 2008; Higuera et al. 2010a), and to identify peaks in charcoal, which were interpreted as fire episodes. The analysis involved interpolating CHAR values to a constant sampling resolution, decomposing that record into a background and a peak component using a robust LOWESS, and evaluating peak samples using both the 99^{th} percentile of the modelled noise distribution obtained with a Gaussian mixture model and a peak-screening test. The suitability of the record for peak detection was assessed with the signal-to-noise index (SNI; Kelly et al. 2011). We calculated fire return intervals (FRI) using the screened peak record.

We used change-point analysis to determine significant changes in biomass burning and test the potential effect of sedimentation rates on change-point detection (Finsinger et al. 2018).

To test the simultaneity between fire and erosion events, thereby allowing identification of high-severity local catchment fires (Chileen et al. 2020), we used Event Coincidence Analysis (ECA; Siegmund et al. 2017). We determined erosion events as (i) peaks of magnetic susceptibility, which respond to increases in minerogenic input that often follow fire events as a result of erosion, and to in-washing of secondary ferromagnetic minerals that are formed when soils with a high concentration of convertible Fe are heated (Thompson and Oldfield 1986; Millspaugh and Whitlock 1995), and (ii) peaks of *Cenococcum geophilum* Fr. sclerotia influx, whose abundances are linked to soil erosion (Van Geel 1978). The two datasets were analysed with a custom-made computer code (R Core Team 2020) in a similar way to the CHAR record to statistically identify distinct peaks. We performed the ECA using two binary event time series (CHAR peaks and erosion peaks), a lag of 8 years, and a tolerance window 8-48 years that detects erosion events within 10-50 years of fire episodes, and tested the significance based on the assumption of independent and sparse Poisson processes (α=0.05).

To identify leads and lags between fire activity (macroscopic charcoal influx values) and vegetation and land-use change (pollen percentages and dung-fungi spores' influx), we used cross-correlation analyses (Green 1981;

Tinner et al. 1999; Valsecchi et al. 2008). We performed the analyses for two time intervals that show different intensity of human pressure: 970-1350 CE (higher pressure); 1600 CE to the present (lower pressure). Within the selected time intervals, the sampling resolution was relatively stable (32±3 and 21±3 years between samples, respectively). The cross-correlations' span was restricted to one-fourth of the sample number *N* (lag number ≤ *N*/4).

Results

Present vegetation composition and forest structure

The forest includes plots characterized by large trees (up to 148 cm of DBH; Fig. 2) and by a high CWD volume (up to 791.6 $m^3 ha^{-1}$; Fig. 3). Plots having a complex horizontal and vertical structure are present as shown by high volume of living trees (V; up to 1781.9 $m^3 ha^{-1}$) and high values of structural diversity indices (G_{BA} up to 0.8) (Table 1). CWD consists mostly of logs (65%) and snags (33%) and rarely stumps (2%). Although beech is the species with the highest overall stems density, beech trees are generally smaller than fir and spruce trees.

The HCA (Fig. S2) identified three forest structural types (FST) that differ significantly from each other (Table 1; Fig. 3). Their overlap on the land-cover type map that we obtained through remote-sensing analysis (Fig. 1; see ESI1 Table S5 for assessment of accuracies) shows that FST1 plots predominantly occur in the beech-dominated outer part of the forest. These plots are dominated by small and mostly multi-stemmed beech trees (DBH generally <40 cm from single stools), and have negligible amounts of CWD, and low BA and density of conifers and other deciduous species. We found an inactive charcoal kiln in one of these plots, and cut stumps in two plots. FST2 and FST3 plots are in a 957-ha conifer-dominated area (34% of the core area) and are dominated by fir (FST3) and predominantly co-dominated by fir and spruce (FST2). FST2 also includes a plot dominated by sycamore maple. CWD and dead to live wood ratio values are significantly higher, and BA and density of beech are significantly lower than in FST1 plots.

The indices of structural diversity (DBH_{SD}, H_{SD}, G_{DBH}, G_{BA}) indicate that plots in the inner part of the forest are structurally more heterogeneous than those in the outer part. FST2 plots have the highest species and structural diversity (Table 1) as they consist of large fir and spruce trees (up to 148 cm in DBH), and small to intermediate beech trees (mostly 10-65 cm in DBH). In FST3 plots, spruce trees are extremely rare, and the prevalent species are fir (intermediate to large diametric classes, up to 115 cm) and beech (small to intermediate diametric classes). Moreover, the DBH_{mean} and volume are significantly lower and the amount of CWD and dead to live wood ratio

values are significantly higher. Regeneration of spruce is very scarce in all plots, while regeneration of fir and beech is significantly higher in FST1 and FST3, respectively.

Median cost of access is lower for FST1 plots in the outer part of the forest (Fig. 3). Cost of access is significantly and positively correlated to BA of fir (Spearman's ρ=0.43, P<0.001) and negatively to BA of beech (Spearman's ρ=-0.36, P <0.01). Positive significant correlations of cost of access are also found with CWD amount (Spearman's ρ=0.44, P<0.001), dead to live wood ratio (Spearman's ρ=0.38, P<0.001) and heterogeneity as described by the DBH standard deviation (Spearman's ρ=0.29, P<0.05) and Gini indices (Spearman's ρ=0.35 for G_{DBH} and 0.30 for G_{BA}, P<0.01).

The difference among forest structures is also supported by the textural analysis of the forest canopy (Figs S3a-c), which are finer and more homogeneous in the outer part, whereas more complex and heterogeneous canopies, probably arising from gap dynamics, are common in the inner part. Most (99%) of the detected gaps occur in the conifer-dominated area. Gap sizes are highly variable (mean: 210 m^2; range: 3.33-5636 m^2) and their distribution is right-skewed (76% of gaps <200 m^2, only 2% >1000 m^2).

Long-term environmental changes

The sediment core spans the past *c.* 1000 years (Fig. S4a). The reliability of the chronology in its most recent part is confirmed by the first occurrence of *Ambrosia* pollen around 1920 CE (Fig. 4). Sediment deposition time (Fig. S4b) varies little (3-8 years cm^{-1}; median=4.4 years cm^{-1}). Sediments deposited before 1300 CE are lighter in colour than the darker-brown detritus gyttja deposited thereafter (see ESI1 for further details on sediment composition and the chronology).

The pollen record (Fig. 4, see ESI1 Fig. S5-S6 for more detailed pollen and macrofossil diagram) was divided into three statistically significant assemblage zones at 123.5 and 52 cm depth (*c*. 1600 and 1850 CE, respectively). However, to better illustrate the long-term vegetation changes we additionally selected a non-significant pollen zone boundary at 171.5 cm (*c*. 1350 CE).

The lowermost pollen assemblages (950-1150 CE) of zone 1a are characterized by decreasing abundance of tree pollen (from 80% to 40%), particularly pollen of conifers (*Abies*, *Pinus sylvestris*-type and *Picea*) and of fern spores (e.g. *Athyrium filix-femina*), which grow in fresh and shaded understorey environments (Ellenberg 2009). The continuous finds of pollen and plant macrofossils of the half-shade demanding *Sambucus* from 950 to 1150 CE indicate the presence of clearings. The transition to a land-use phase (1150-1350 CE), which is demonstrated

by high abundance of primary anthropogenic indicators and adventives as well as by *Sporormiella* and *Tilletia* spores, is marked by a short-term expansion of *Rhamnus* (1050-1150 CE).

Anthropogenic indicators and herb pollen abundances distinctly decrease around 1350 CE (onset of zone 1b) indicating a sudden abandonment of pasture and cultivation. Higher abundance of arboreal pollen percentages in conjunction with angiosperm leaves and fern spores indicates the establishment of broadleaf trees with a fern understorey. *Picea* was present in the surroundings, as shown by stomata and plant-macrofossil finds. The pollen record shows the expansion of trees and shrubs that typically colonise abandoned pastures (*Sambucus*, *Betula*, *Alnus, Ulmus* and *Acer*). A century later (around 1450 CE) pollen, stomata and plant-macrofossils of shade-tolerant *Abies* and *Fagus* trees increased. The development of a mixed woodland was interrupted by a short-term and milder land-use phase (1500-1600 CE), as suggested by the slight rise of primary and secondary anthropogenic indicators, fire-adapted *Pteridium* and upland herbs.

Local conifer populations collapsed during this second land-use phase (onset of zone 2: 1590 CE) and a *Fagus*-dominated forest gradually established around the site. Pollen and plant macrofossils indicate that light-demanding woody species (*Corylus*, *Betula*) expanded faster than the shade-tolerant *Fagus,* which peaked around 100 years later (1700 CE). *Fagus* and *Fraxinus* pollen as well as their plant macrofossils markedly decreased between 1760 and 1850 CE in conjunction with a slight rise in *Sporormiella* and *Veratrum* spores, which indicates a third land-use phase characterised by grazing.

During the past 170 years (zone 3; 1850 CE to present), a *Fagus*-dominated forest type developed with increasing abundance of *Ulmus*, *Alnus, Fraxinus* and *Acer*, low abundance of anthropogenic indicators, and decreasing abundance of pioneer trees and shrubs (*Corylus* and *Betula*). Tree cover has been highest since 1950 CE.

Macroscopic charcoal concentration values ranged between 0 and 271 (median = 34 pieces cm^{-3}). Charcoal counts and charcoal areas are significantly correlated (R^2=0.91, P<0.001). Peak analyses based on different parameters are highly comparable among one another with mean SNI values generally higher than the critical threshold (Table S6; Figs S8-S9). The periods of shorter fire-return intervals (1000-1150 CE, FRI=25 years; 1460-1520 CE, FRI=60 years; and 1730-1810 CE, FRI=75 years) occur predominantly during phases of high biomass burning (1000-1030, 1340-1730, and 1730-1850 CE, Figs 5 and S10). A large majority (75%, P=0.05) of the erosion events occurred 10-50 years after fire episodes (Fig. S11). This is the case for erosion events occurring at the onset of the Middle Ages (1050 CE), towards the end of the Middle Ages (1500-1550 CE), and during the 20th-century. The coincidence between fire episodes and erosion events suggests that these were triggered by higher-severity

catchment fires, whereas fire episodes occurring during the medieval land-use phase (1050-1150 CE) and around 1800 CE were of lower intensity or occurred outside the catchment.

We used cross-correlation analyses (Fig. 6) to explore leads and lags between fire activity and vegetation and land-use change separately for (i) the Middle Ages when human pressure was higher (970-1350 CE; zone 1b), and (ii) the more recent centuries (1600 CE to the present; zones 2-3) when human pressure was lower and the forest was protected. Significant negative correlation coefficients ($P<0.05$) between charcoal-accumulation rates (CHAR) and arboreal pollen, *Abies*, *Picea* and *Fagus* in the Middle Ages indicate that fires contributed considerably to the decline of late seral species. We found the highest correlation coefficients when CHAR lagged primary indicators and dung spores by 30 years, consistently with mechanisms of charcoal taphonomy leading to delayed deposition at a coring location (Duffin et al., 2008; Higuera et al., 2010). Thus, the significant positive correlations between CHAR and primary anthropogenic indicators and dung spores at negative lags support the hypothesis of human-driven fires used to create open areas for agriculture and grazing.

For the time interval when human pressure was lower (1600 CE to the present) arboreal pollen is negatively correlated with fire, and primary anthropogenic indicators are positively correlated with fire at lag 0, thus corroborating the link between cultivation and fire. Dung fungi also show positive significant correlations with fire, though the highest coefficients are found at positive lags, suggesting a delayed increase of grazing ca. 60 years after fire activity rises. By contrast, in this time interval the correlation coefficients between CHAR and *Abies*, *Picea* and *Fagus* are not significant. However, *Corylus* and *Betula* show positive significant correlations ahead of the charcoal peaks (at lags -4 and -5), suggesting that these light-demanding pioneer species acted as fire precursors, and *Fraxinus* shows a negative significant correlation at lag 0. It thus seems likely that land-use and fires mainly occurred in gaps within the overall *Fagus*-dominated forest.

Discussion

Current forest structure within the old-growth stands and the surrounding forest

Our extensive ground surveys and the detailed remote-sensing analyses show that the Biogradska Gora forest is characterised by a large compositional and structural variability. We detected a fine-scale variability due to gap dynamics within the conifer-dominated matrix in the inner part, which allow the recruitment of more light-demanding species, like sycamore maple, in larger gaps (Nagel et al. 2014). In addition to this fine-scale variability, we identified three forest structural types (FSTs) showing different degrees of old-growthness (Fig. 3) that are unevenly distributed within the forest (Fig. 1). The structural and compositional variability supports the notion

that plots placed in a limited area that is considered representative of old-growth characteristics may lead to an overestimation of average old-growthness (Peck et al. 2015; Carrer et al. 2018).

The structure in the inner part of the forest (FST2 and FST3) is comparable to that of other mixed old-growth forests such as Perućica, Lom, and Jani in Bosnia-Herzegovina (Motta et al. 2011, 2015b, a; Keren et al. 2014, 2020; Zenner et al. 2015; Chivulescu et al. 2020), both in terms of variables assessed previously (BA, V, and CWD) by Motta et al. (2015a) as well as in terms of dead to live wood ratio and structural diversity (Table 1, Figs 2 and 3). Moreover, the heterogeneous texture of the forest canopy with small-scale gaps also shows that the conifer-dominated stands in the inner part of the forest likely had the time to develop typical old-growth attributes (Spies and Franklin 1988; Wirth et al. 2009).

The HCA confirms prior studies showing that the old-growth forest includes two structural types, their main differences being the rarity of spruce (Motta et al. 2015a) and significantly higher dead biomass (CWD and dead to live wood ratio values) in the fir-dominated FST3 plots (Fig. 3). Because spruce is rare in these plots, their significantly higher amount of dead biomass could be linked to higher spruce mortality. This would fit with the persisting decline of the spruce population, as indicated by its extremely low seedling regeneration and the absence of spruce saplings in all plots (Table 1). The decline of spruce may agree with evidence showing that at the southern boundary of its distributional range populations of the cold-adapted spruce are more vulnerable to drought than fir and beech (Hanewinkel et al. 2013; Zang et al. 2014). In agreement with this, in the Dinaric Alps spruce dominated stands are common in karst depressions and sinkholes where temperature inversions cause significantly colder microclimates (Nagel et al. 2017). Conversely, the low spruce regeneration could be explained by the scarcity of expanded gaps, as spruce is less shade tolerant than beech and fir (Stancioiu and O'Hara 2006a) and beech is the main gap filler species in a small-scale disturbance regime (Petritan et al. 2014) typical of old-growth forests.

In the beech-dominated outer part of the forest (FST1) CWD consists mostly of logs with a lesser number of snags, as often observed in old-growth stands (Nilsson et al. 2003) and as observed in the inner part of the forest. However, the FST1 plots have substantially lower CWD values than FST2 and FST3 plots. While this is relatively unsurprising given that broadleaved trees produce a lower deadwood accumulation (Harmon et al. 2004) due to their lower height and volume, and their deadwood decays faster than deadwood of conifer species (e.g. 20-40 years for Fagus, and within 58-191 years for conifer snags on moist sites; Vacek et al. 2015; Hararuk et al. 2020), these plots also have substantially lower CWD values than other European beech-dominated old-growth forests (Burrascano et al. 2013; Meyer et al. 2021). Interestingly, CWD and dead to live wood ratio values are closer to those found in currently managed forests or in those recently withdrawn from regular management (Motta et al.

2015b). Moreover, the lower structural diversity of these plots and the finer texture of the forest canopy rather reflect a homogeneous structure and even-aged cohorts.

Stand-scale long-term vegetation dynamics, land-use changes and disturbances by fire

Despite the importance of pollen loading from regional sources, the proportion of pollen loading coming to the 0.05-ha-pond in the beech-dominated area from the relevant pollen source area (200-300 m for such sites) is adequate to reflect local vegetation composition (Sugita 1994; Hofstetter et al. 2006). This is also supported by the coherence between the pollen and the plant-macrofossil and stomata records (Fig. 7) that are generally dispersed over substantially shorter distances than pollen (Birks and Bjune 2010; Ammann et al. 2014). Similarly, while the source area of macroscopic charcoal particles can be relatively large (up to 30-50 km; Oris et al. 2014; Adolf et al. 2018), both empirical and simulated data support the assumption that charcoal peaks most accurately reflect fire episodes within 1–3 km of coring sites (Higuera et al. 2010b). Moreover, the coincidence of peaks in charcoal and erosion-indicators helped us to pinpoint the occurrence of local higher-severity catchment fire episodes (Fig. 7). Thus, our palaeoecological record predominantly documents local-scale vegetation dynamics, land-use and fire occurrence for the currently beech-dominated outer part of the forest.

During the Middle Ages, tree cover was substantially lower and cereal crop cultivation and cattle herding were more widespread than today (Fig. 7). Finds of spores of common bunt (*Tilletia sp.*) suggest that pathogens affected cultivated crops, as these pathogens can cause devastating yield reductions by up to 50% (Kiesselbach and Lyness 1939). Bunt was one of the most severe diseases of winter wheat (*Triticum aestivum* L.) in the Middle Ages (Gaudet and Menzies 2012) and harvest failures were important factors for social vulnerability, particularly for people living in rural areas in pre-industrial economies (Pfister and Brázdil 2006). These constraints on crop cultivation favoured abandonment of the fields surrounding the pond, thereby causing the tree cover increase around 1350 CE when the Black Death pandemic rapidly spread and substantially reduced population density (Green 2014; Luterbacher et al. 2020).

Despite setbacks due to the occurrence of more moderate and transient local land-use phases with the use of fire, tree cover increased after 1350 CE. This trajectory markedly contrasts with decreasing tree cover due to intensifying land-use since the 15th-16th century (Fig. 7) documented for nearby Bosnia-Herzegovina (Prokoško Jezero; Dörfler 2013), the coastal region of Albania-Montenegro (Shkodra Jezero; Sadori et al. 2015), as well as for elsewhere in Europe (Fyfe et al. 2015; Conedera et al. 2017), and as suggested by models (Kaplan et al. 2009). The absence of evidence for intensifying land-use after the 15th century at Biogradska Gora could be due to the

411 transition to cooler temperatures and the beginning of the Little Ice Age (LIA), which may have discouraged
412 cultivation and pasturing in the valley. Indeed, years with unusually cold spring seasons during the LIA had serious
413 consequences on grain harvests and on cattle in the meridional Balkans and in Serbia (Xoplaki et al. 2001; Mrgic
414 2018). An alternative, or additional, explanation could be the small pollen source area, which predominantly
415 captured pollen from the surrounding expanding beech stand despite ongoing land use on the hilltops where
416 meadows still exist today. Regardless, the tree-cover increase and decreasing land-use pressure that started around
417 1500-1600 CE suggests that the 19th century's formal protection of the forest eventually took advantage of the pre-
418 existing situation, supporting the view that historical land-use pressure is a significant predictor for the occurrence
419 of primary and old-growth forests (Sabatini et al. 2018).
420 The longer continuity of the conifer-dominated old-growth stands is currently not supported by firm evidence due
421 to the lack of palaeoecological sites in that area. On one hand, these stands may have developed after the 15th-16th
422 century, when land-use declined. This would fit with age estimates of deadwood showing that trees up to 400-500
423 years old occurred in the conifer-dominated stands (Motta et al. 2015a). On the other hand, the presence of stomata
424 and plant macrofossils before the 15th-16th century in the currently beech-dominated outer part of the forest (Fig.
425 7) rather supports the hypothesis that the area of fir and spruce-dominated old-growth forest was reduced during
426 the Middle Ages. In Central and in southern European mountains fir declined several millennia earlier (Büntgen
427 et al. 2014; Morales-Molino et al. 2020) than at Biogradska Gora, and it is plausible to hypothesise that fir declined
428 earlier in more accessible mountain areas. The higher cost of access may have prevented human activities in the
429 old-growth forest, and land-use activities were probably limited to the outer part of the forest, as observed at
430 Biogradska Gora (Černjavski 1937) and as is often the case for protected ecosystems (Hansen and DeFries 2007).
431 Fires either did not propagate into the inner part of the forest, or their severity was not high enough to affect the
432 fire-sensitive fir population. Overall, this supports the notions that human pressure played an important role for
433 the small extent of old-growth forests (Nagel et al. 2017; Sabatini et al. 2018) and that buffer zones are key for
434 protecting old-growth forests (Barredo et al. 2021).
435
436 ***Legacies of past human activities***
437 Forest composition in the surroundings of the small pond shifted from a mixed fir-spruce-broadleaf stand to one
438 dominated by beech at the transition to cooler LIA temperatures and in conjunction to a land-use pressure decline
439 around 1500-1600 CE (Fig. 7). Analogous expansions of beech at the expense of fir are well documented in mid-
440 late Holocene pollen records from central-southern Europe, and evidence suggests that despite the two species

currently sharing large parts of the ecological niche (Houston Durrant et al. 2016; Mauri et al. 2016), beech became more competitive after the decline of *Abies alba* and with the onset of cooler and moister summers and human fire disturbance (Vescovi et al. 2010; Morales-Molino et al. 2020). While it is difficult to disentangle the effects of climate and land-use, it seems likely that land-use and fire occurrence probably played an important role in driving the vegetation shift. The conifer population was strongly reduced due to increased local fire activity (Fig. 6) in conjunction with land-use during the Middle Ages, and the local conifer population finally collapsed in 1500 CE when two higher-severity local fires occurred at the onset of a moderate land-use phase (Fig. 7). This is in line with a wealth of evidence showing that conspicuous canopy gaps (from fires and land-use) can cause a reshuffling of the dominant tree species in mixed fir, beech and spruce forests. Spruce, for instance, does not survive or re-sprout after high severity fires (Niklasson et al. 2010; Feurdean et al. 2019) despite bearing traits promoting fires (high resin content, ladder canopy structure) and being able to persist with a low to moderate fire severity (Feurdean et al. 2017). Similarly, both large-infrequent and small-frequent fires lead to a rapid local extinction of the fire-intolerant *Abies* (Tinner et al. 2013). By contrast, human activities and disturbance by fire can favour the spread of beech at the stand level (Bradshaw and Lindbladh 2005; Tinner and Lotter 2006). Beech quickly re-sprouts and regenerates successfully after small or intermediate human and natural disturbances (windthrow, cutting, fire; Motta et al. 2011; Nagel et al. 2014; Maringer et al. 2016). Importantly, beech regenerates faster than fir and spruce in canopy gaps and overstorey releases (Stancioiu and O'Hara 2006b; Bolte et al. 2014). Additionally, beech encircles competitors and fills gaps after disturbances (Pretzsch and Schütze 2005; Bolte et al. 2014) as it rapidly takes advantage of more favourable light conditions due to higher morphological plasticity of foliage and crown structures (Dieler and Pretzsch 2013). Thus, frequent small or intermediate-scale disturbances (Delarze et al. 1992), such as those created by land-use associated with the use of fire, can promote beech (Bolte et al. 2014). An additional explanation could involve clear-cutting and extraction of conifer timber in stands that are accessible for harvest (Büntgen et al. 2014). Other forms of land-use, such as coppicing, also could have favoured beech to obtain firewood or wood charcoal, as observed elsewhere in marginal areas of coniferous woodland in Central Europe (Winkler 1963). Coppicing and clear-cutting practices developed greatly due to increasing wood demand and demographic growth in the 16th-17th centuries and after 1850 CE (McEvedy and Jones 1978). At Biogradska Gora, these practices are attested to by multi-stemmed beech trees and traces of charcoal kilns in some plots in the more accessible outer part of the forest.

The protected old-growth forest of Biogradska Gora should be sufficiently large (>1000 ha) to buffer the effects of small-scale natural disturbances (Sabatini et al. 2018). Moreover, population density in mountain areas is

predicted to decrease over the 21st century in eastern Europe due to abandonment of pastoral and agricultural activities (Wu et al. 2015). This may also be beneficial to the majority of primary and old-growth forests that are substantially smaller (<100 ha) (Sabatini et al. 2018). However, old-growth forests may be at risk due to predicted environmental changes. For instance, despite the rare natural fire occurrence and the much greater importance of other disturbance agents (bark beetle outbreaks, windthrows; Nagel et al. 2017), forest fires are predicted to increase in the region, which could potentially become a new fire-prone area (Krawchuk et al. 2009; Wu et al. 2015). Warmer and drier conditions that may lead to increased fires will also likely affect vegetation structure modifying fuel type, fuel load and therefore fire intensity and spread, increasing mortality rates. For instance, as fir is known to be more drought tolerant than beech (Morales-Molino et al. 2020) its population may recover if other disturbances (e.g. fires) do not prevent the expansion of this fire-sensitive tree species.

Conclusions

The multi-proxy palaeoecological records (pollen, spores, stomata, macrofossils, macroscopic charcoal, and magnetic susceptibility) coupled with the extensive survey of current forest structures and with the map of land-cover types from the Biogradska Gora forest provide new insights into the long-term vegetation dynamics of old-growth forests in the montane zone of the Dinaric Mountains. The stand-scale palaeoecological records show that human activities (agriculture, and pastures) as well as fires, which are rare today in these forest types (Nagel et al. 2017) reduced the area of fir and spruce-dominated forest during the Middle Ages. Despite the local land-use decline 500-400 years ago and the early protection of the forest 140 years ago, the legacies of past land-use activities are still visible, as the conifer-dominated mixed forest in the inner part of the valley has more old-growth characteristics than the almost pure beech forest in the outer part. However, the continuity and increase of tree cover in the outer part of the forest since the 16th century markedly contrasts with the widespread high conversion rates to agriculture and forest exploitation elsewhere in Europe during the past millennium (Kaplan et al. 2009; Fyfe et al. 2015; Birks and Tinner 2016), thereby supporting the view that historical land-use pressure played an important role for the small extent and the continuity of disturbance-sensitive *A. alba* and *P. abies*-dominated old-growth stands.

Our study shows that combining stand-scale long-term ecological records with assessments of contemporary forest structure can generate valuable insights (Foster et al. 1996), as the structures and spatial patterns of ecosystems are often a result of legacy effects arising from complex interactions between natural and human disturbances

(McLachlan et al. 2000; Vale 2002; Willis and Birks 2006; Whitlock et al. 2018), which is critical information for guiding forest management and conservation measures (Conedera et al. 2017).

Figures and Figure captions

Fig. 1 Map showing the distribution of land-cover types in the Biogradska Gora National Park obtained through the remote-sensing analysis of Pléiades satellite images. Circles indicate the locations of field-survey plots (colour-coded by forest structural type, FST). The star shows the location of the palaeoecological site. The inset shows the study area location in a larger spatial context

Fig. 2 Cumulative diametric (DBH) class distributions in the field-survey plots grouped by forest structural type

Fig. 3 Boxplots illustrating differences among forest structural types in the Biogradska Gora forest. Whiskers represent the first and third quartiles of the distributions, and the horizontal black lines are referred to the median values. Y-axis indicates values of coarse woody debris (CWD), dead to live wood ratio, Tree diameter diversity index (TDD), Gini index referred to the basal area (G_{BA}), diameter standard deviation (DBH_{SD}), basal area (BA) and path distance

Figure 4 Pollen percentage (continuous curves) and plant macrofossil (black bar plots) concentrations diagram of selected taxa from the small pond in the Biogradska Gora valley. Horizontal continuous and dotted lines represent significant and non-significant pollen zone boundaries, respectively. See ESI1 for more detailed pollen and plant-macrofossil diagrams

Fig. 5 Comparison between erosion and charcoal-derived fire history. a) Magnetic susceptibility (MS); b) Macroscopic charcoal accumulation rate (CHAR) interpolated to 8 years (black), charcoal background modelled using a 500-year smoothing window (grey line), while red line indicates final positive and negative threshold values for peaks identification. Identified CHAR peaks are marked with "+" symbols. Grey shaded areas refer to periods of relatively stable biomass burning as determined by the change-point analysis (the darker the shade the higher the mean CHAR values are). See ESI1 for results obtained with other user-determined parameters (interpolation and smoothing-window widths). c) Fire return interval (FRI) values. Vertical continuous and dotted lines represent significant and non-significant pollen zone boundaries, respectively

Fig. 6 Cross-correlograms of charcoal accumulation rates (CHAR), selected pollen percentages and dung-fungi spores' influxes for two phases of different intensity of human pressure. (i) The Middle Ages when human pressure was higher (970-1350 CE; <1350 CE) and (ii) the more recent centuries when human pressure was lower (1600

CE to the present; > 1600 CE). Horizontal axis shows the lag. One lag is equal to *c.* 30 years for phase (i) and to *c.* 20 years for phase (ii). Vertical axis: correlation coefficients; dashed horizontal lines: 95% confidence limits

Fig. 7 Comparison between vegetation dynamics (pollen and non-pollen palynomorphs: filled areas; plant macrofossils: black barplots; stomata: full circles), macroscopic charcoal (CHAR) inferred fire history (red crosses: higher-severity fire events), and magnetic-susceptibility (MS) inferred erosion history (black and blue crosses: erosion events) at Biogradska Gora, and warm-season (May-August, MAMJJA) temperature (see ESI1 for further details). The bottom panels show the tree cover at Prokoško Jezero, Bosnia-Herzegovina (Dörfler, 2013) and the abundance of total closed forest in Europe (Fyfe et al., 2015)

Acknowledgements

We are grateful to D. D'Aprile for help during fieldwork, to I. Figueral, L. Bouby and F. Wagner-Cremer for help with identification of plant-macrofossil, wood and charcoal pieces and *Fagus* stomata, and to R. Marzano, D. Ascoli, C. Urbinati, D. McKey, E. Ilardi, and D. Barbaro for discussions. We thank the Biogradska Gora National Park for granting permission to collect sediments and perform the field surveys.

Declarations

Funding: EC was financially supported by the Land Environment Resources and Health (L.E.R.H.) doctoral course of the University of Padova (DOR1957359/19; “Disturbi naturali in foresta: Studio su una old-growth forest dei Balcani”) and by the Fondazione Ing. Aldo Gini. This work was supported by public funds received in the framework of GEOSUD, a project (ANR-10-EQPX-20) of the program "Investissements d'Avenir" managed by the French National Research Agency.

Availability of data and material: All data will be made publicly available upon acceptance. The palaeoecological data (pollen, spores, stomata, plant macrofossils, macroscopic charcoal, and magnetic susceptibility) will be uploaded to the Neotoma database (DOI: 10.21233/XYZZ-XYZZ) through the European Pollen Database. The forest structure and composition data will be uploaded to Figshare (figshare.com).

Code availability (software application or custom code): The custom-made computer code in R will be available on GitHub (https://github.com/wfinsinger) and archived in Zenodo (https://zenodo.org/) upon acceptance.

Authors’ contributions

WF, RM, EL, MG, and EC conceived the ideas and designed methodology; EC, WF, EL, MG, NM, FM, LP collected the data; EC, WF and DM analysed the data; EC, WF, and EL led the writing of the manuscript; MG, RM, LP, NM, FM, MC, VS, IB reviewed the manuscript. All authors contributed critically to the drafts and gave final approval for publication.

References

Adolf C, Wunderle S, Colombaroli D, et al (2018) The sedimentary and remote-sensing reflection of biomass burning in Europe. Glob Ecol Biogeogr 27:199–212. https://doi.org/10.1111/geb.12682

Ammann B, Knaap WO van der, Lang G, et al (2014) The potential of stomata analysis in conifers to estimate presence of conifer trees: examples from the Alps. Veg Hist Archaeobotany 23:249–264. https://doi.org/10.1007/s00334-014-0431-9

Baker AG, Bhagwat SA, Willis KJ (2013) Do dung fungal spores make a good proxy for past distribution of large herbivores? Quat Sci Rev 62:21–31. https://doi.org/10.1016/j.quascirev.2012.11.018

Barredo JI, Brailescu C, Teller A, et al (2021) Mapping and assessment of primary and old-growth forests in Europe. Luxembourg

Bauhus J, Puettmann K, Messier C (2009) Silviculture for old-growth attributes. For Ecol Manag 258:525–537. https://doi.org/10.1016/j.foreco.2009.01.053

Behre K-E (1981) The interpretation of anthropogenic indicators in pollen diagrams. Pollen Spores 23:225–245

Bennett KD (2008) Psimpoll v. 4.26

Bennett KD (1996) Determination of the number of zones in a biostratigraphical sequence. New Phytol 132:155–170

Birks HH, Birks HJB (2000) Future uses of pollen analysis must include plant macrofossils. J Biogeogr 27:31–35

Birks HH, Bjune AE (2010) Can we detect a west Norwegian tree line from modern samples of plant remains and pollen? Results from the DOORMAT project. Veg Hist Archaeobotany 19:325–340. https://doi.org/10.1007/s00334-010-0256-0

Birks HJB (2019) Contributions of Quaternary botany to modern ecology and biogeography. Plant Ecol Divers 12:189–385. https://doi.org/10.1080/17550874.2019.1646831

Birks HJB, Gordon AD (1985) Numerical Methods in Quaternary Pollen Analysis. Academic Press, London

Birks HJB, Tinner W (2016) Past forests of Europe. In: San-Miguel-Ayanz J, de Rigo D, Caudullo G, et al. (eds) European Atlas of Forest Tree Species. Publications Office of the European Union, Luxembourg, pp 36–39

Blaauw M, Christen JA (2011) Flexible Paleoclimate Age-Depth Models Using an Autoregressive Gamma Process. Bayesian Anal 6:457–474. https://doi.org/10.1214/11-BA618

Bolte A, Hilbrig L, Grundmann BM, Roloff A (2014) Understory dynamics after disturbance accelerate succession from spruce to beech-dominated forest—the Siggaboda case study. Ann For Sci 71:139–147. https://doi.org/10.1007/s13595-013-0283-y

Bradshaw RHW, Lindbladh M (2005) Regional spread and stand-scale establishment of Fagus sylvatica and Picea abies in Scandinavia. Ecology 86:1679–1686

599 Brillouin L (1956) Science and Information Theory. Academic Press, New York (USA)

600 Buchwald E (2005) A hierarchical terminology for more or less natural forests in relation to sustainable
601 management and biodiversity conservation. FAO, Rome, 17–19 January 2005, p 17

602 Büntgen U, Tegel W, Kaplan JO, et al (2014) Placing unprecedented recent fir growth in a European-wide and
603 Holocene-long context. Front Ecol Environ 12:100–106. https://doi.org/10.1890/130089

604 Burrascano S, Keeton WS, Sabatini FM, Blasi C (2013) Commonality and variability in the structural attributes
605 of moist temperate old-growth forests: A global review. For Ecol Manag 291:458–479.
606 https://doi.org/10.1016/j.foreco.2012.11.020

607 Carrer M, Castagneri D, Popa I, et al (2018) Tree spatial patterns and stand attributes in temperate forests: The
608 importance of plot size, sampling design, and null model. For Ecol Manag 407:125–134.
609 https://doi.org/10.1016/j.foreco.2017.10.041

610 Černjavski P (1937) Zur Kenntnis der Glaziation und des Buchenwaldes bei Biogradsko Jezero in Montenegro.
611 Bull Inst Jard Bot Univ Beogr 4:24–41

612 Chileen BV, McLauchlan KK, Higuera PE, et al (2020) Vegetation response to wildfire and climate forcing in a
613 Rocky Mountain lodgepole pine forest over the past 2500 years. The Holocene 30:1493–1503.
614 https://doi.org/10.1177/0959683620941068

615 Chivulescu S, Ciceu A, Leca S, et al (2020) Development phases and structural characteristics of the Penteleu-
616 Viforâta virgin forest in the Curvature Carpathians. IForest - Biogeosciences For 13:389.
617 https://doi.org/10.3832/ifor3094-013

618 Conedera M, Colombaroli D, Tinner W, et al (2017) Insights about past forest dynamics as a tool for present and
619 future forest management in Switzerland. For Ecol Manag 388:100–112.
620 https://doi.org/10.1016/j.foreco.2016.10.027

621 Conedera M, Tinner W, Neff C, et al (2009) Reconstructing past fire regimes: methods, applications, and
622 relevance to fire management and conservation. Quat Sci Rev 28:555–576.
623 https://doi.org/10.1016/j.quascirev.2008.11.005

624 Csontos P, Vitalos M, Barina Z, Kiss L (2010) Early distribution and spread of *Ambrosia artemisiifolia* in
625 Central and Eastern Europe. Bot Helvetica 120:75–78. https://doi.org/10.1007/s00035-010-0072-2

626 Čurović M, Stešević D, Medarević M, et al (2011) Ecological and structural characteristics of monodominant
627 montane beech forests in the National park Biogradska Gora, Montenegro. Arch Biol Sci 63:429–440

628 Davis OK (1987) Spores of the dung fungus *Sporormiella*: increased abundance in historic sediments and before
629 Pleistocene megafaunal extinction. Quat Res 28:290–294

630 Delarze R, Calderari D, Hainard P (1992) Effects of fire on forest dynamics in southern Switzerland. J Veg Sci
631 3:55–60

632 Deza-Araujo M, Morales-Molino C, Tinner W, et al (2020) A critical assessment of human-impact indices based
633 on anthropogenic pollen indicators. Quat Sci Rev 236:106291.
634 https://doi.org/10.1016/j.quascirev.2020.106291

635 Diaci J (ed) (1999) Virgin forests and forest reserves in Central and East European countries: history, present
636 status and future development: proceedings of the invited lecturers' reports presented at the COST E4
637 management committee and working groups meeting in Ljubljana, Slovenia, Ljubljana, 25-28 April,
638 1998. Dept. of Forestry and Renewable Forest Resources, Ljubljana

639 Dieler J, Pretzsch H (2013) Morphological plasticity of European beech (*Fagus sylvatica* L.) in pure and mixed-
640 species stands. For Ecol Manag 295:97–108. https://doi.org/10.1016/j.foreco.2012.12.049

641 Dörfler W (2013) Prokoško Jezero: An environmental record from a subalpine lake in Bosnia-Herzegovina. In:
642 Müller J, Rassmann K, Hofmann R (eds) Okolište 1 – Untersuchungen einer spätneolithischen
643 Siedlungskammer in Zentralbosnien. Habelt Verlag, Bonn, pp 311–340

644 Ellenberg H (2009) Vegetation ecology of Central Europe, 4th Edition. Cambridge University Press

645 Elsen PR, Monahan WB, Dougherty ER, Merenlender AM (2020) Keeping pace with climate change in global
646 terrestrial protected areas. Sci Adv 6:eaay0814. https://doi.org/10.1126/sciadv.aay0814

647 Feurdean A, Florescu G, Vannière B, et al (2017) Fire has been an important driver of forest dynamics in the
648 Carpathian Mountains during the Holocene. For Ecol Manag 389:15–26.
649 https://doi.org/10.1016/j.foreco.2016.11.046

650 Feurdean A, Tonkov S, Pfeiffer M, et al (2019) Fire frequency and intensity associated with functional traits of
651 dominant forest type in the Balkans during the Holocene. Eur J For Res 138:1049–1066.
652 https://doi.org/10.1007/s10342-019-01223-0

653 Fick SE, Hijmans RJ (2017) WorldClim 2: new 1-km spatial resolution climate surfaces for global land areas. Int
654 J Climatol 37:4302–4315. https://doi.org/10.1002/joc.5086

655 Finsinger W, Fevre J, Orbán I, et al (2018) Holocene fire-regime changes near the treeline in the Retezat Mts.
656 (Southern Carpathians, Romania). Quat Int 477:94–105. https://doi.org/10.1016/j.quaint.2016.04.029

657 Finsinger W, Morales-Molino C, Gałka M, et al (2017) Holocene vegetation and fire dynamics at Crveni Potok,
658 a small mire in the Dinaric Alps (Tara National Park, Serbia). Quat Sci Rev 167:63–77.
659 https://doi.org/10.1016/j.quascirev.2017.04.032

660 Finsinger W, Tinner W (2020) New insights on stomata analysis of European conifers 65 years after the
661 pioneering study of Werner Trautmann (1953). Veg Hist Archaeobotany 29:393–406.
662 https://doi.org/10.1007/s00334-019-00754-1

663 Foster DR, Orwlg DA, McLachlan JS (1996) Ecological and conservation insights from reconstructive studies of
664 temperate old-growth forests. Trends Ecol Evol 11:419–424. https://doi.org/10.1016/0169-
665 5347(96)10047-1

666 Fyfe RM, Woodbridge J, Roberts N (2015) From forest to farmland: pollen-inferred land cover change across
667 Europe using the pseudobiomization approach. Glob Change Biol 21:1197–1212.
668 https://doi.org/10.1111/gcb.12776

669 Garbarino M, Lingua E, Weisberg PJ, et al (2013) Land-use history and topographic gradients as driving factors
670 of subalpine *Larix decidua* forests. Landsc Ecol 28:805–817. https://doi.org/10.1007/s10980-012-9792-
671 6

672 Gaudet D, Menzies J (2012) Common bunt of wheat: an old foe remains a current threat. In: Sharma I (ed)
673 Disease Resistance in Wheat. CABI, pp 220–235

674 Gini C (1912) Variabilità e Mutabilità (Variability and Mutability). C. Cuppini, Bologna, Italy

675 Green DG (1981) Time Series and Postglacial Forest Ecology. Quat Res 15:265–277

676 Green MH (2014) Taking "Pandemic" Seriously: Making the Black Death Global. Mediev Globe 1:27–62

677 Grizonnet M, Michel J, Poughon V, et al (2017) Orfeo ToolBox: open source processing of remote sensing
678 images. Open Geospatial Data Softw Stand 2:15. https://doi.org/10.1186/s40965-017-0031-6

679 Hanewinkel M, Cullmann DA, Schelhaas M-J, et al (2013) Climate change may cause severe loss in the
680 economic value of European forest land. Nat Clim Change 3:203–207.
681 https://doi.org/10.1038/nclimate1687

682 Hansen AJ, DeFries R (2007) Ecological mechanisms linking protected areas to surrounding lands. Ecol Appl
683 17:974–988. https://doi.org/10.1890/05-1098

684 Hararuk O, Kurz WA, Didion M (2020) Dynamics of dead wood decay in Swiss forests. For Ecosyst 7:36.
685 https://doi.org/10.1186/s40663-020-00248-x

686 Harmon ME, Franklin JF, Swanson FJ, et al (2004) Ecology of coarse woody debris in temperate ecosystems. In:
687 Advances in Ecological Research. Academic Press, pp 59–234

688 Higuera PE, Brubaker LB, Anderson PM, et al (2009) Vegetation mediated the impacts of postglacial climate
689 change on fire regimes in the south-central Brooks Range, Alaska. Ecol Monogr 79:201–219

690 Higuera PE, Gavin DG, Bartlein PJ, Hallett DJ (2010a) Peak detection in sediment–charcoal records: impacts of
691 alternative data analysis methods on fire-history interpretations. Int J Wildland Fire 19:996.
692 https://doi.org/10.1071/WF09134

693 Higuera PE, Whitlock C, Gage JA (2010b) Linking tree-ring and sediment-charcoal records to reconstruct fire
694 occurrence and area burned in subalpine forests of Yellowstone National Park, USA. The Holocene
695 21:327–341. https://doi.org/10.1177/0959683610374882

696 Hofstetter S, Tinner W, Valsecchi V, et al (2006) Lateglacial and Holocene vegetation history in the Insubrian
697 Southern Alps—New indications from a small-scale site. Veg Hist Archaeobotany 15:87–98.
698 https://doi.org/10.1007/s00334-005-0005-y

699 Horvat I, Glavač V, Ellenberg H (1974) Vegetation of Southeast Europe. Gustav Fischer Verlag, Stuttgart

700 Houston Durrant T, de Rigo D, Caudullo G (2016) *Fagus sylvatica* in Europe: distribution, habitat, usage and
701 threats. In: San Miguel-Ayanz J, de Rigo D, Caudullo G, et al. (eds) European Atlas of Forest Tree
702 Species. Publ. Off. EU, Luxembourg, p e012b90+.

703 Kaplan JO, Krumhardt KM, Zimmermann N (2009) The prehistoric and preindustrial deforestation of Europe.
704 Quat Sci Rev 28:3016–3034. https://doi.org/10.1016/j.quascirev.2009.09.028

705 Kelly R, Higuera PE, Barrett CM, Hu FS (2011) A signal-to-noise index to quantify the potential for peak
706 detection in sediment–charcoal records. Quat Res 75:11–17.
707 https://doi.org/10.1016/j.yqres.2010.07.011

708 Keren S, Motta R, Govedar Z, et al (2014) Comparative structural dynamics of the Janj mixed old-growth
709 mountain forest in Bosnia and Herzegovina: Are conifers in a long-term decline? Forests 5:1243–1266.
710 https://doi.org/10.3390/f5061243

711 Keren S, Svoboda M, Janda P, Nagel TA (2020) Relationships between structural indices and conventional stand
712 attributes in an old-growth forest in southeast Europe. Forests 11:4. https://doi.org/10.3390/f11010004

713 Kiesselbach TA, Lyness WE (1939) The effects of stinking smut (Bunt) and seed treatment upon the yield of
714 winter wheat. Hist Res Bull Neb Agric Exp Stn 1913-1993 110:1–25

715 Krawchuk MA, Moritz MA, Parisien M-A, et al (2009) Global pyrogeography: the current and future
716 distribution of wildfire. PLOS ONE 4:e5102. https://doi.org/10.1371/journal.pone.0005102

717 Leibundgut H (1959) Über Zweck und Methodik der Struktur und Zuwachsanalyse von Urwäldern. Schweiz Z
718 Für Forstwes 110:111–124

719 Lindbladh M (1999) The influence of former land-use on vegetation and biodiversity in the boreo-nemoral zone
720 of Sweden. Ecography 22:485–498. https://doi.org/10.1111/j.1600-0587.1999.tb01277.x

721 Luburić V (2016) The introduction of new management measures in protected areas with the aim of improving
722 models of nature protection of Montenegro. PhD, University of Novi Sad

Luterbacher J, Newfield TP, Xoplaki E, et al (2020) Past pandemics and climate variability across the Mediterranean. Euro-Mediterr J Environ Integr 5:46, s41207-020-00197–5. https://doi.org/10.1007/s41207-020-00197-5

Makra L, Juhász M, Béczi R, Borsos E (2005) The history and impacts of airborne *Ambrosia* (Asteraceae) pollen in Hungary. Grana 44:57–64. https://doi.org/10.1080/00173130510010558

Maringer J, Conedera M, Ascoli D, et al (2016) Resilience of European beech forests (*Fagus sylvatica* L.) after fire in a global change context. Int J Wildland Fire 25:699. https://doi.org/10.1071/WF15127

Marlon JR, Bartlein PJ, Carcaillet C, et al (2008) Climate and human influences on global biomass burning over the past two millennia. Nat Geosci 1:697–702. https://doi.org/10.1038/ngeo313

Mauri A, de Rigo D, Caudullo G (2016) *Abies alba* in Europe: distribution, habitat, usage and threats. In: San-Miguel-Ayanz J, de Rigo D, Caudullo G, et al. (eds) European Atlas of Forest Tree Species. Publ. Off. EU, Luxembourg, p e01493b+

Mazurkiewicz-Zapałowicz K, Okuniewska-Nowaczyk I (2015) Mycological and palynological studies of early medieval cultural layers from strongholds in Pszczew and Santok (western Poland). 10

Mazziotta A, Heilmann-Clausen J, Bruun HH, et al (2016) Restoring hydrology and old-growth structures in a former production forest: Modelling the long-term effects on biodiversity. For Ecol Manag 381:125–133. https://doi.org/10.1016/j.foreco.2016.09.028

McEvedy C, Jones R (1978) Atlas of World Population History. Penguin Books, London

McLachlan JS, Foster DR, Menalled F (2000) Anthropogenic ties to late-successional structure and composition in four New England Hemlock stands. Ecology 81:717–733. https://doi.org/10.1890/0012-9658(2000)081[0717:ATTLSS]2.0.CO;2

McMullin RT, Wiersma YF (2019) Out with OLD growth, in with ecological continNEWity: new perspectives on forest conservation. Front Ecol Environ. https://doi.org/10.1002/fee.2016

Meyer P, Aljes M, Culmsee H, et al (2021) Quantifying old-growthness of lowland European beech forests by a multivariate indicator for forest structure. Ecol Indic 125:107575. https://doi.org/10.1016/j.ecolind.2021.107575

Michel J, Youssefi D, Grizonnet M (2015) Stable mean-shift algorithm and Its application to the segmentation of arbitrarily large remote sensing images. IEEE Trans Geosci Remote Sens 53:952–964. https://doi.org/10.1109/TGRS.2014.2330857

Millspaugh SH, Whitlock C (1995) A 750-year fire history based on lake sediment records in central Yellowstone National Park, USA. The Holocene 5:283–292. https://doi.org/10.1177/095968369500500303

Morales-Molino C, Steffen M, Samartin S, et al (2020) Long-term responses of mediterranean mountain forests to climate change, fire and human activities in the northern Apennines (Italy). Ecosystems. https://doi.org/10.1007/s10021-020-00587-4

Motta R, Berretti R, Castagneri D, et al (2011) Toward a definition of the range of variability of central European mixed *Fagus – Abies – Picea* forests: the nearly steady-state forest of Lom (Bosnia and Herzegovina). Can J For Res 41:1871–1884. https://doi.org/10.1139/x11-098

Motta R, Garbarino M, Berretti R, et al (2015a) Structure, spatio-temporal dynamics and disturbance regime of the mixed beech–silver fir–Norway spruce old-growth forest of Biogradska Gora (Montenegro). Plant Biosyst - Int J Deal Asp Plant Biol 149:966–975. https://doi.org/10.1080/11263504.2014.945978

Motta R, Garbarino M, Berretti R, et al (2015b) Development of old-growth characteristics in uneven-aged forests of the Italian Alps. Eur J For Res 134:19–31. https://doi.org/10.1007/s10342-014-0830-6

Mrgic J (2018) Intemperate weather in violent times – narratives from the Western Balkans during the Little Ice Age (17-18th centuries). Cuad Investig Geográfica 44:137. https://doi.org/10.18172/cig.3380

Nagel TA, Mikac S, Dolinar M, et al (2017) The natural disturbance regime in forests of the Dinaric Mountains: A synthesis of evidence. For Ecol Manag 388:29–42. https://doi.org/10.1016/j.foreco.2016.07.047

Nagel TA, Svoboda M, Kobal M (2014) Disturbance, life history traits, and dynamics in an old-growth forest landscape of southeastern Europe. Ecol Appl 24:663–679

Niklasson M, Zin E, Zielonka T, et al (2010) A 350-year tree-ring fire record from Białowieża Primeval Forest, Poland: implications for Central European lowland fire history. J Ecol 98:1319–1329. https://doi.org/10.1111/j.1365-2745.2010.01710.x

Nilsson SG, Niklasson M, Hedin J, et al (2003) Erratum to "Densities of large living and dead trees in old-growth temperate and boreal forests." For Ecol Manag 178:355–370. https://doi.org/10.1016/S0378-1127(03)00084-7

Nowaczyk NR (2001) Logging of magnetic susceptibility. In: Tracking Environmental Change Using Lake Sediments. Volume 1: Basin Analysis, Coring, and Chronological Techniques. Kluwer Academic Publishers, Dordrecht, The Netherlands, pp 155–170

Öder V, Petritan AM, Schellenberg J, et al (2021) Patterns and drivers of deadwood quantity and variation in mid-latitude deciduous forests. For Ecol Manag 487:118977. https://doi.org/10.1016/j.foreco.2021.118977

Oris F, Ali AA, Asselin H, et al (2014) Charcoal dispersion and deposition in boreal lakes from 3 years of monitoring: Differences between local and regional fires. Geophys Res Lett 41:6743–6752. https://doi.org/10.1002/2014GL060984

Peck JE, Commarmot B, Hobi ML, Zenner EK (2015) Should reference conditions be drawn from a single 10 ha plot? Assessing representativeness in a 10,000 ha old-growth European beech forest. Restor Ecol 23:927–935. https://doi.org/10.1111/rec.12258

Petritan IC, Marzano R, Petritan AM, Lingua E (2014) Overstory succession in a mixed *Quercus petraea–Fagus sylvatica* old growth forest revealed through the spatial pattern of competition and mortality. For Ecol Manag 326:9–17. https://doi.org/10.1016/j.foreco.2014.04.017

Pfister C, Brázdil R (2006) Social vulnerability to climate in the "Little Ice Age": an example from Central Europe in the early 1770s. Clim Past 2:115–129. https://doi.org/10.5194/cp-2-115-2006

Pluskowski A, Seetah K (2006) The animal bones from the 2004 excatavation at Stari Bar, Montenegro. In: Gelichi S (ed) The Archaeology of an abandoned town. The 2005 Project in Stari Bar. All'Insegna del Giglio, Florence, pp 97–111

Pretzsch H, Schütze G (2005) Crown allometry and growing space efficiency of Norway spruce (*Picea abies* [L.] Karst.) and European beech (*Fagus sylvatica* L.) in pure and mixed stands. Plant Biol Stuttg Ger 7:628–639. https://doi.org/10.1055/s-2005-865965

R Core Team (2020) R: A language and environment for statistical computing. R Foundation for Statistical Computing, Vienna, Austria

Reimer PJ, Bard E, Bayliss A, et al (2013) IntCal13 and Marine13 radiocarbon age calibration curves 0-50,000 years cal BP

Rouvinen S, Kuuluvainen T (2005) Tree diameter distributions in natural and managed old *Pinus sylvestris*-dominated forests. For Ecol Manag 208:45–61. https://doi.org/10.1016/j.foreco.2004.11.021

Sabatini FM, Burrascano S, Keeton WS, et al (2018) Where are Europe's last primary forests? Divers Distrib 24:1426–1439. https://doi.org/10.1111/ddi.12778

Sabatini FM, Keeton WS, Lindner M, et al (2020) Protection gaps and restoration opportunities for primary forests in Europe. Divers Distrib 26:1646–1662. https://doi.org/10.1111/ddi.13158

Sadori L, Giardini M, Gliozzi E, et al (2015) Vegetation, climate and environmental history of the last 4500 years at lake Shkodra (Albania/Montenegro). The Holocene 25:435–444. https://doi.org/10.1177/0959683614561891

Schütz J-P, Saniga M, Diaci J, Vrška T (2016) Comparing close-to-nature silviculture with processes in pristine forests: lessons from Central Europe. Ann For Sci 73:911–921. https://doi.org/10.1007/s13595-016-0579-9

Siegmund JF, Siegmund N, Donner RV (2017) CoinCalc —A new R package for quantifying simultaneities of event series. Comput Geosci 98:64–72. https://doi.org/10.1016/j.cageo.2016.10.004

Spies TA, Franklin JF (1988) Old growth and forest dynamics in the Douglas-fir region of Western Oregon and Washington. Nat Areas J 8:190–201

Stancioiu PT, O'Hara KL (2006a) Morphological plasticity of regeneration subject to different levels of canopy cover in mixed-species, multiaged forests of the Romanian Carpathians. Trees 20:196–209. https://doi.org/10.1007/s00468-005-0026-2

Stancioiu PT, O'Hara KL (2006b) Regeneration growth in different light environments of mixed species, multiaged, mountainous forests of Romania. Eur J For Res 125:151–162. https://doi.org/10.1007/s10342-005-0069-3

Stijovic A (2017) Bazna studija o sumama u Nacionalnom parku Biogradska Gora (Podloga za upravljanje sumama). JP Nacionalni parkovi Crne Gore

Sugita S (1994) Pollen representation of vegetation in Quaternary sediments - theory and method in patchy vegetation. J Ecol 82:881–897

Sun W, Chen B, Messinger D (2014) Nearest-neighbor diffusion-based pan-sharpening algorithm for spectral images. Opt Eng 53:013107. https://doi.org/10.1117/1.OE.53.1.013107

Thompson R, Oldfield F (1986) Environmental magnetism. Allen & Unwin Ltd, London

Tinner W, Colombaroli D, Heiri O, et al (2013) The past ecology of *Abies alba* provides new perspectives on future responses of silver fir forests to global warming. Ecol Monogr 83:419–439. https://doi.org/10.1890/12-2231.1

Tinner W, Hubschmid P, Wehrli M, et al (1999) Long-term forest fire ecology and dynamics in southern Switzerland. J Ecol 87:273–289

Tinner W, Lotter AF (2006) Holocene expansions of *Fagus silvatica* and *Abies alba* in Central Europe: where are we after eight decades of debate? Quat Sci Rev 25:526–549

UNESCO (2010) UNESCO Global Strategy: the Man and the Biosphere Programme. In: UNESCO World Herit. Cent. https://whc.unesco.org/en/tentativelists/5569/. Accessed 17 May 2021

Vacek S, Vacek Z, Bílek L, et al (2015) The dynamics and structure of dead wood in natural spruce-beech forest stand – a 40 year case study in the Krkonoše National Park. Dendrobiology 73:21–32. https://doi.org/10.12657/denbio.073.003

Vale TR (2002) The Pre-European landscape of the United States. In: Vale TR (ed) Fire, native peoples, and the natural landscape. Island Press, Washington, D.C.

Valsecchi V, Finsinger W, Tinner W, Ammann B (2008) Testing the influence of climate, human impact, and fire on the Holocene population expansions of *Fagus sylvatica* in the southern Prealps (Italy). The Holocene 18:603-614. doi: 10.1177/0959683608089213

851 Van Geel B (1978) A palaeoecological study of Holocene peat bog sections in Germany and The Netherlands,
852 based on the analysis of pollen, spores and macro- and microscopic remains of fungi, algae,
853 cormophytes and animals. Rev Palaeobot Palynol 25:1–120. https://doi.org/10.1016/0034-
854 6667(78)90040-4

855 Vescovi E, Ammann B, Ravazzi C, Tinner W (2010) A new Late-glacial and Holocene record of vegetation and
856 fire history from Lago del Greppo, northern Apennines, Italy. Veg Hist Archaeobotany 19:219–233.
857 https://doi.org/10.1007/s00334-010-0243-5

858 Weiner J, Solbrig OT (1984) The meaning and measurement of size hierarchies in plant populations. Oecologia
859 61:334–336. https://doi.org/10.1007/BF00379630

860 Whitlock C, Colombaroli D, Conedera M, Tinner W (2018) Land-use history as a guide for forest conservation
861 and management. Conserv Biol 32:84–97. https://doi.org/10.1111/cobi.12960

862 Whitlock C, Larsen C (2001) Charcoal as a fire proxy. In: Smol JP, Birks HJB, Last WM, Last WM (eds)
863 Terrestrial, Algal, and Siliceous Indicators. Kluwer Academic Publishers, Dordrecht, The Netherlands,
864 pp 75–97

865 Willis KJ, Birks HJB (2006) What is natural? The need for a long-term perspective in biodiversity conservation.
866 Science 314:1261–1265

867 Winkler E (1963) Beiträge zur Klimatologie hochalpiner Lagen der Zentralalpen. Berichte
868 Naturwissenschaftlich-Med Ver Innsbr 53:209–223

869 Wirth C, Messier C, Bergeron Y, et al (2009) Old-growth forest definitions: a pragmatic view. In: Wirth C,
870 Gleixner G, Heimann M (eds) Old-Growth Forests. Springer Berlin Heidelberg, Berlin, Heidelberg, pp
871 11–33

872 Wright MN, Ziegler A (2017) ranger: A fast implementation of random forests for high dimensional data in C++
873 and R. J Stat Softw 77:1–17. https://doi.org/10.18637/jss.v077.i01

874 Wu M, Knorr W, Thonicke K, et al (2015) Sensitivity of burned area in Europe to climate change, atmospheric
875 CO_2 levels, and demography: A comparison of two fire-vegetation models: Projected future burned area
876 in Europe. J Geophys Res Biogeosciences 120:2256–2272. https://doi.org/10.1002/2015JG003036

877 Xoplaki E, Maheras P, Luterbacher J (2001) Variability of climate in meridional Balkans during the periods
878 1675-1717 and 1780-1830 and its impact on human life. Clim Change 48:581–615.
879 https://doi.org/10.1023/A:1005616424463

880 Zang C, Hartl-Meier C, Dittmar C, et al (2014) Patterns of drought tolerance in major European temperate forest
881 trees: climatic drivers and levels of variability. Glob Change Biol 20:3767–3779.
882 https://doi.org/10.1111/gcb.12637

883 Zenner EK, Sagheb-Talebi K, Akhavan R, Peck JE (2015) Integration of small-scale canopy dynamics smoothes
884 live-tree structural complexity across development stages in old-growth Oriental beech (*Fagus*
885 *orientalis* Lipsky) forests at the multi-gap scale. For Ecol Manag 335:26–36.
886 https://doi.org/10.1016/j.foreco.2014.09.023

887

888

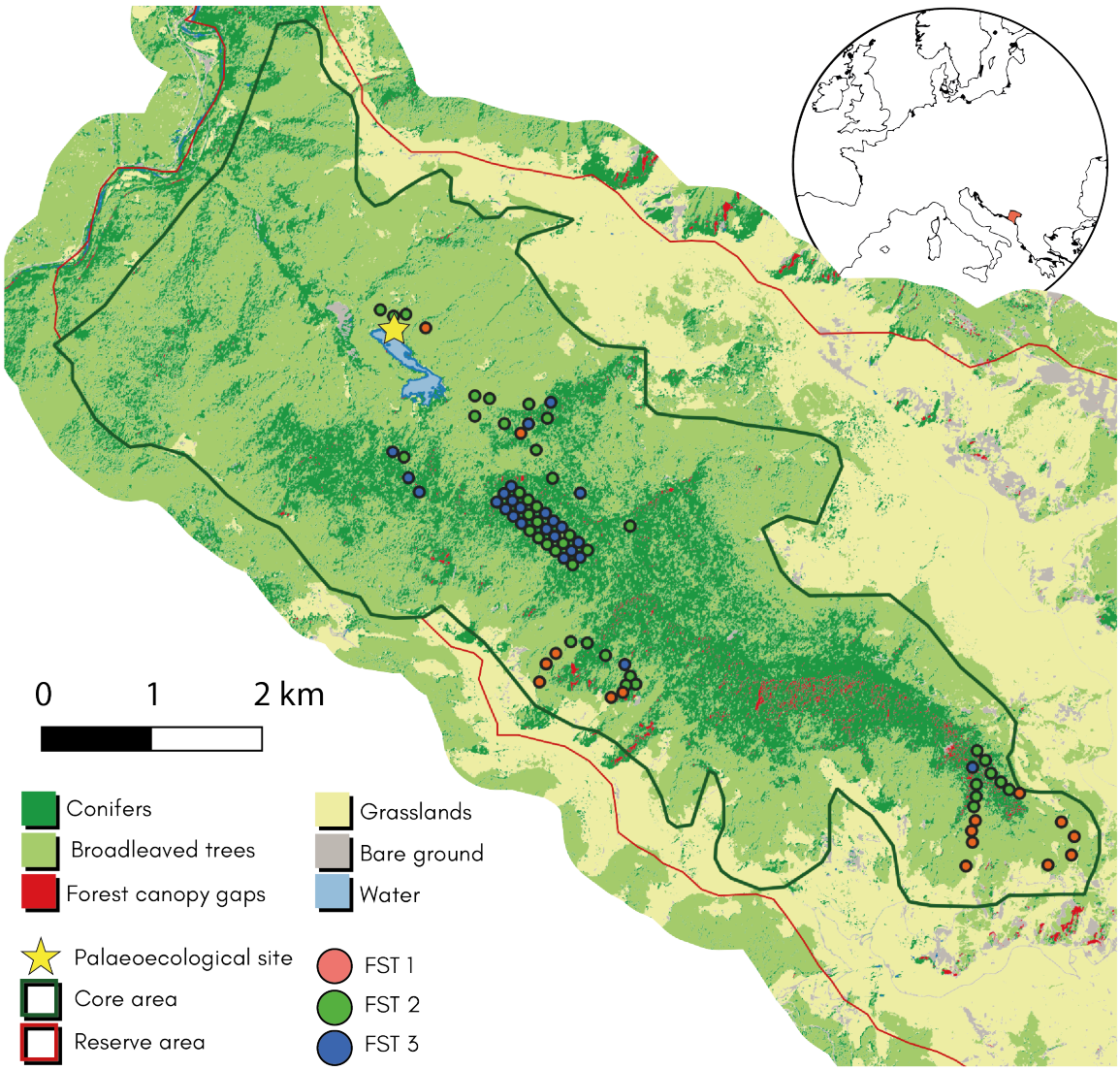
0
1
2 km
Conifers
Broadleaved trees
Forest canopy gaps
Palaeoecological site
Core area
Reserve area
Grasslands
Bare ground
Water
FST 1
FST 2
FST 3

889

890

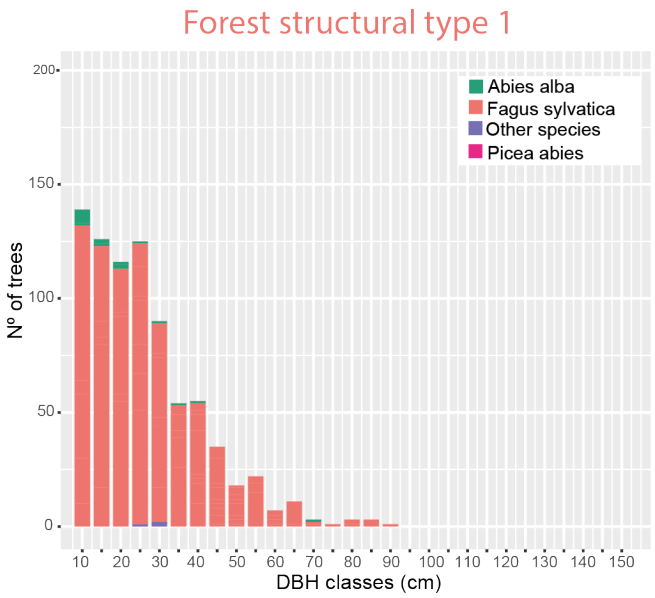
Forest structural type 1
Abies alba
Fagus sylvatica
Other species
Picea abies
Nº of trees
DBH classes (cm)

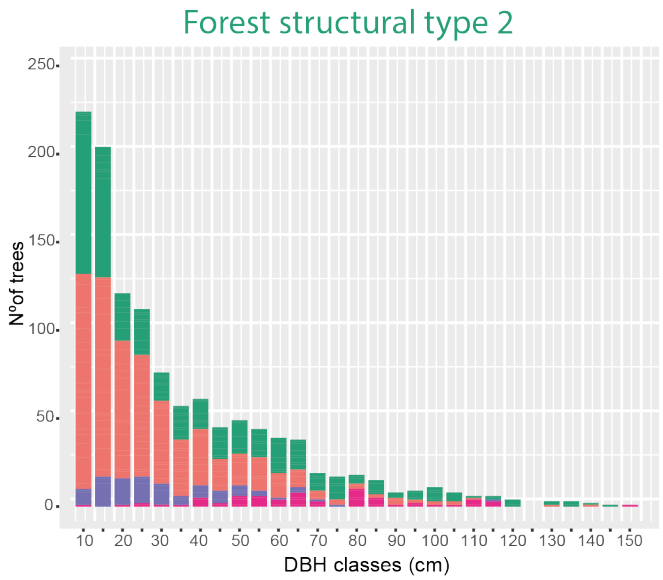
Forest structural type 2
Nºof trees
DBH classes (cm)

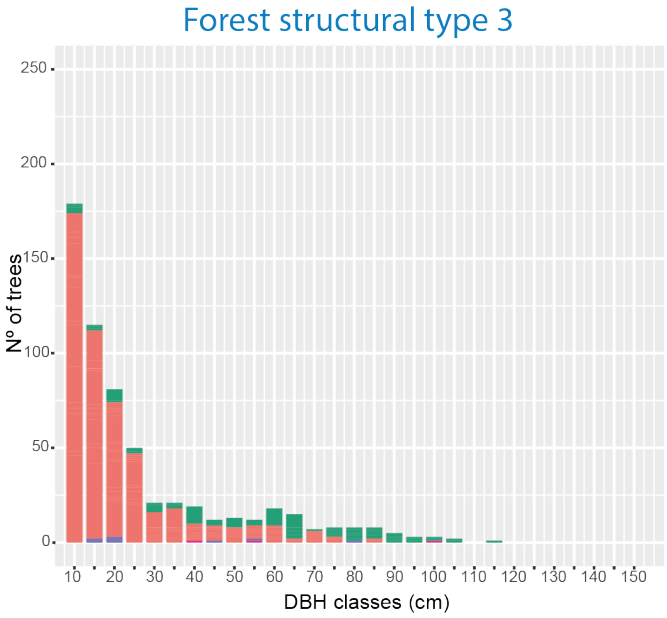
Forest structural type 3
Nº of trees
DBH classes (cm)

891

892

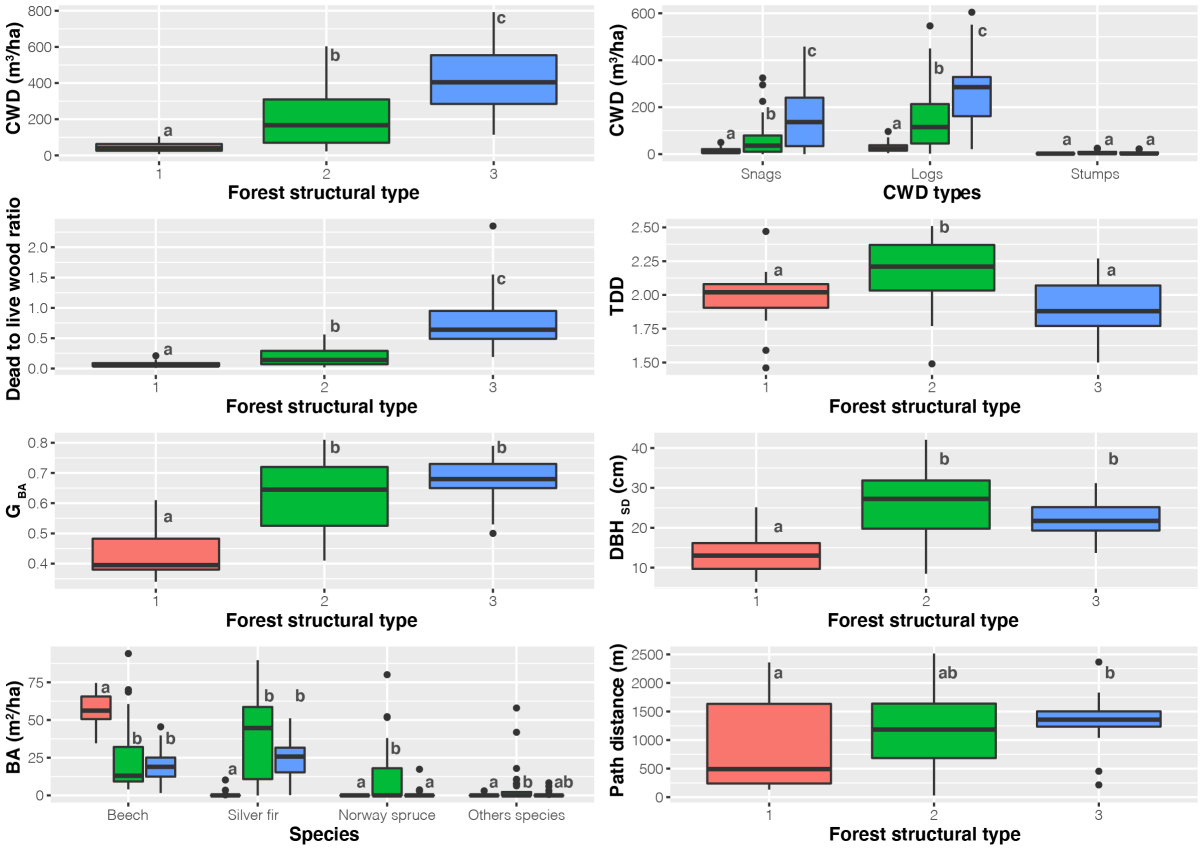
CWD (m³/ha)
Forest structural type
CWD types
Snags
Logs
Stumps
Dead to live wood ratio
TDD
G BA
DBH SD (cm)
BA (m²/ha)
Species
Beech
Silver fir
Norway spruce
Others species
Path distance (m)

893

894

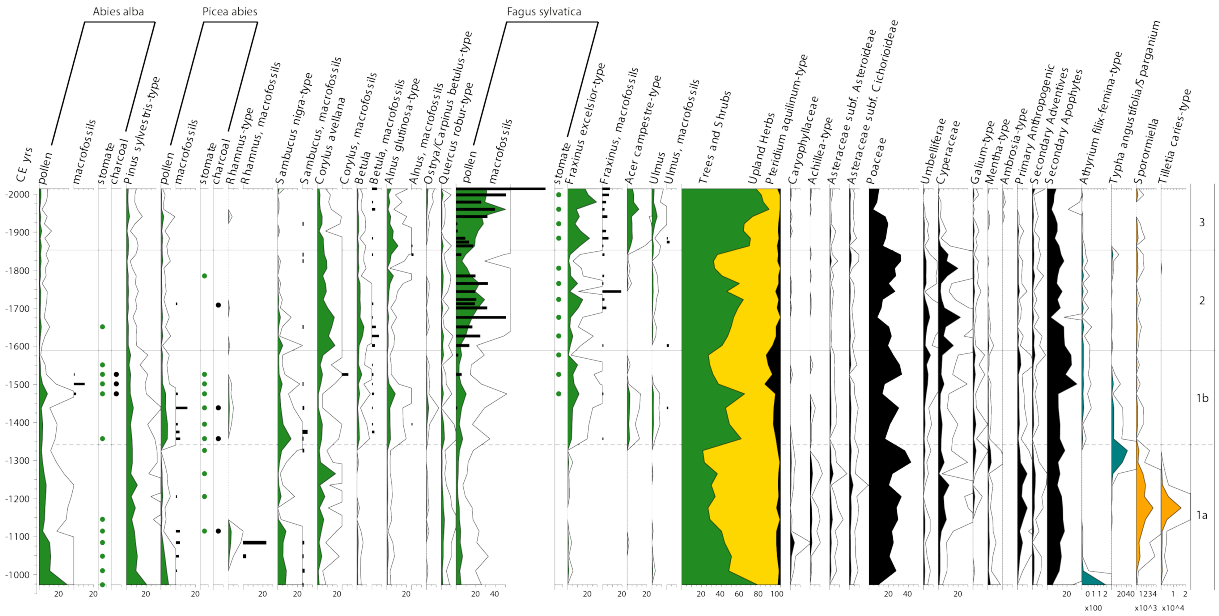
Abies alba
Picea abies
Fagus sylvatica
C.E. yrs
pollen
macrofossils
stomata
charcoal
Pinus sylvestris-type
pollen
macrofossils
stomata
charcoal
R.hamnus-type
R.hamnus, macrofossils
Sambucus nigra-type
Sambucus, macrofossils
Corylus avellana
Corylus, macrofossils
Betula
Betula, macrofossils
Alnus glutinosa-type
Alnus, macrofossils
Ostrya/Carpinus betulus-type
Quercus robur-type
pollen
macrofossils
stomata
Fraxinus excelsior-type
Fraxinus, macrofossils
Acer campestre-type
Ulmus
Ulmus, macrofossils
Trees and Shrubs
Upland Herbs
Pteridium aquilinum-type
Caryophyllaceae
Achillea-type
Asteraceae subf. Asteroideae
Asteraceae subf. Cichorioideae
Poaceae
Umbelliferae
Cyperaceae
Galium-type
Mentha-type
Ambrosia-type
Primary Anthropogenic
Secondary Adventives
Secondary Apophytes
Athyrium filix-femina-type
Typha angustifolia,S.parganium
Sparganiella
Tilletia caries-type
-2000
-1900
-1800
-1700
-1600
-1500
-1400
-1300
-1200
-1100
-1000
3
2
1b
1a
x100
x10^3
x10^4

895

896

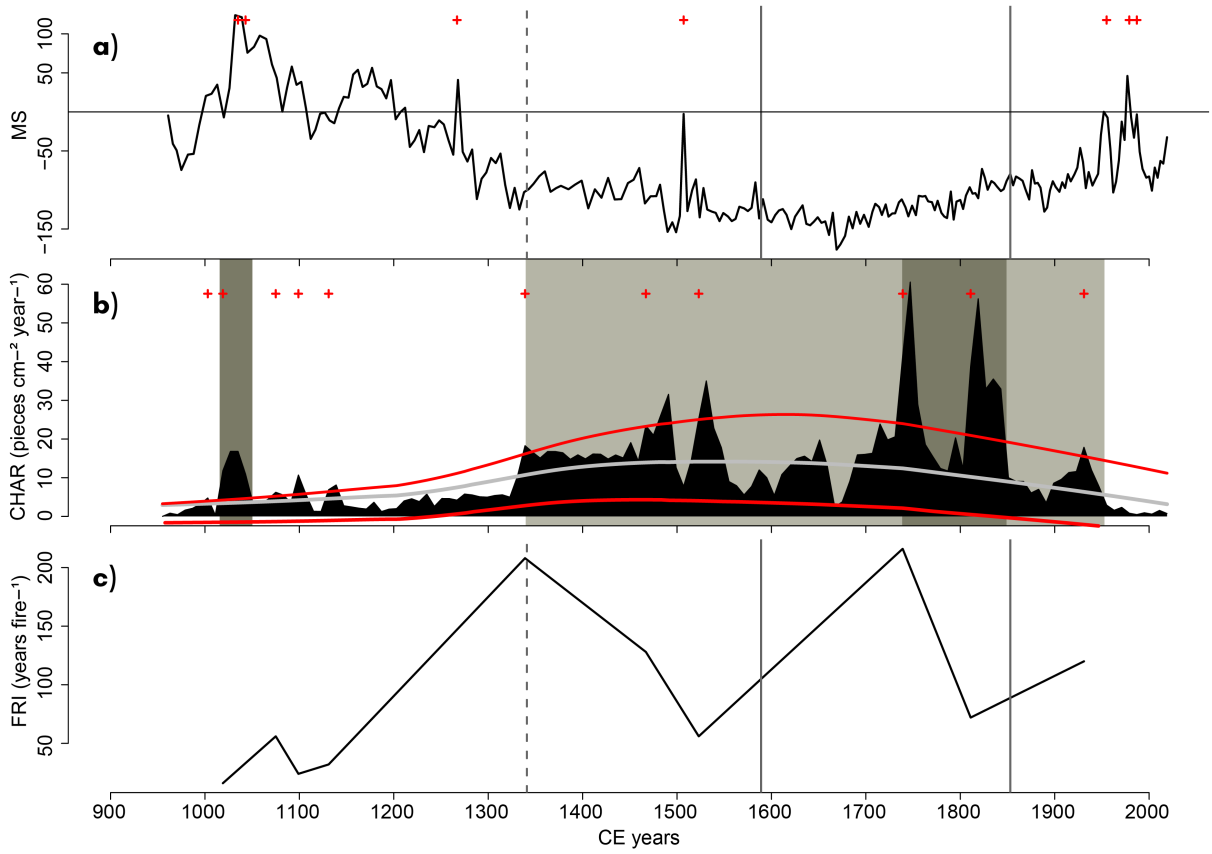
a)
MS
100
50
−50
−150
b)
CHAR (pieces cm−2 year−1)
60
50
40
30
20
10
0
c)
FRI (years fire−1)
200
150
100
50
900
1000
1100
1200
1300
1400
1500
1600
1700
1800
1900
2000
CE years

897

898

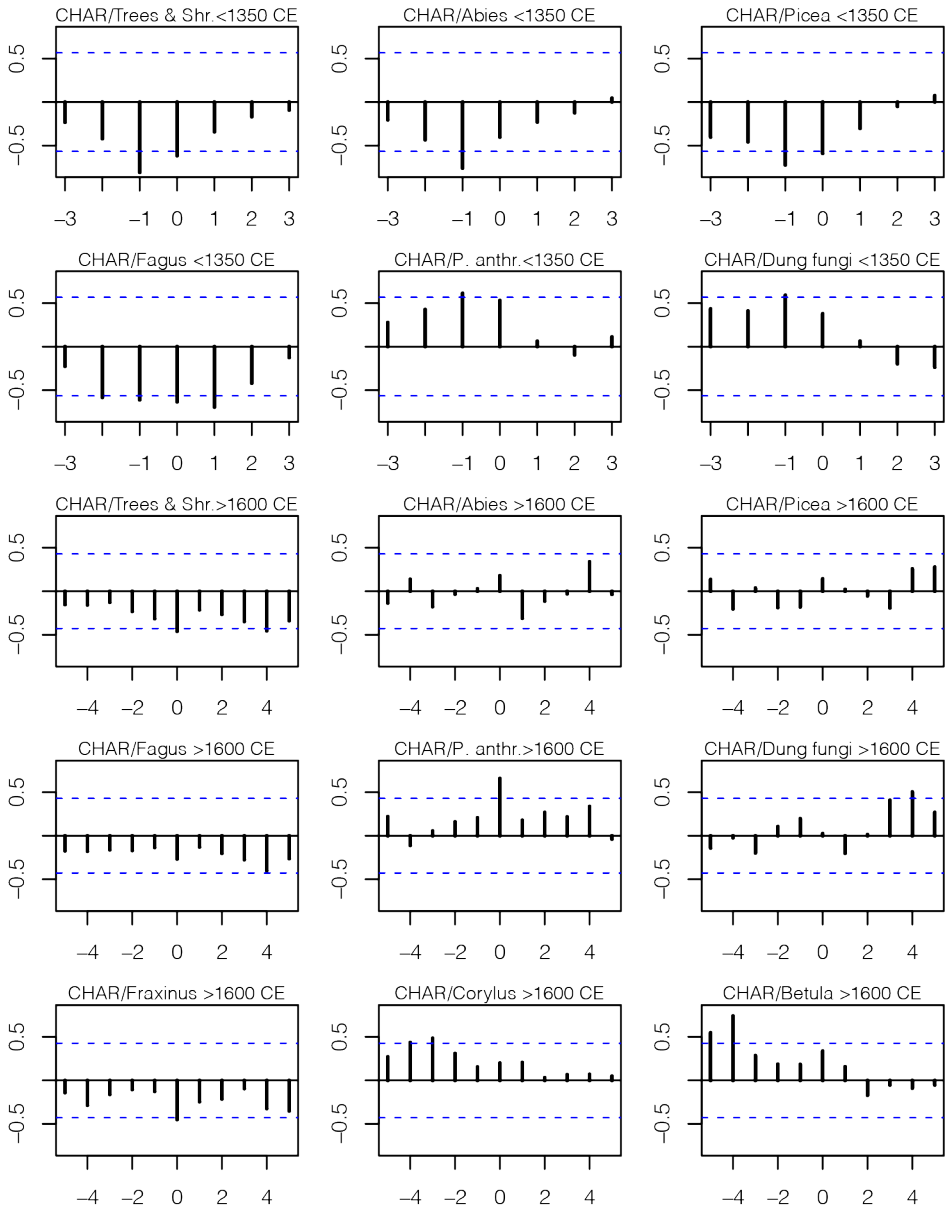
CHAR/Trees & Shr.<1350 CE
CHAR/Abies <1350 CE
CHAR/Picea <1350 CE
CHAR/Fagus <1350 CE
CHAR/P. anthr.<1350 CE
CHAR/Dung fungi <1350 CE
CHAR/Trees & Shr.>1600 CE
CHAR/Abies >1600 CE
CHAR/Picea >1600 CE
CHAR/Fagus >1600 CE
CHAR/P. anthr.>1600 CE
CHAR/Dung fungi >1600 CE
CHAR/Fraxinus >1600 CE
CHAR/Corylus >1600 CE
CHAR/Betula >1600 CE
0.5
−0.5
−3 −1 0 1 2 3
−4 −2 0 2 4

899

900

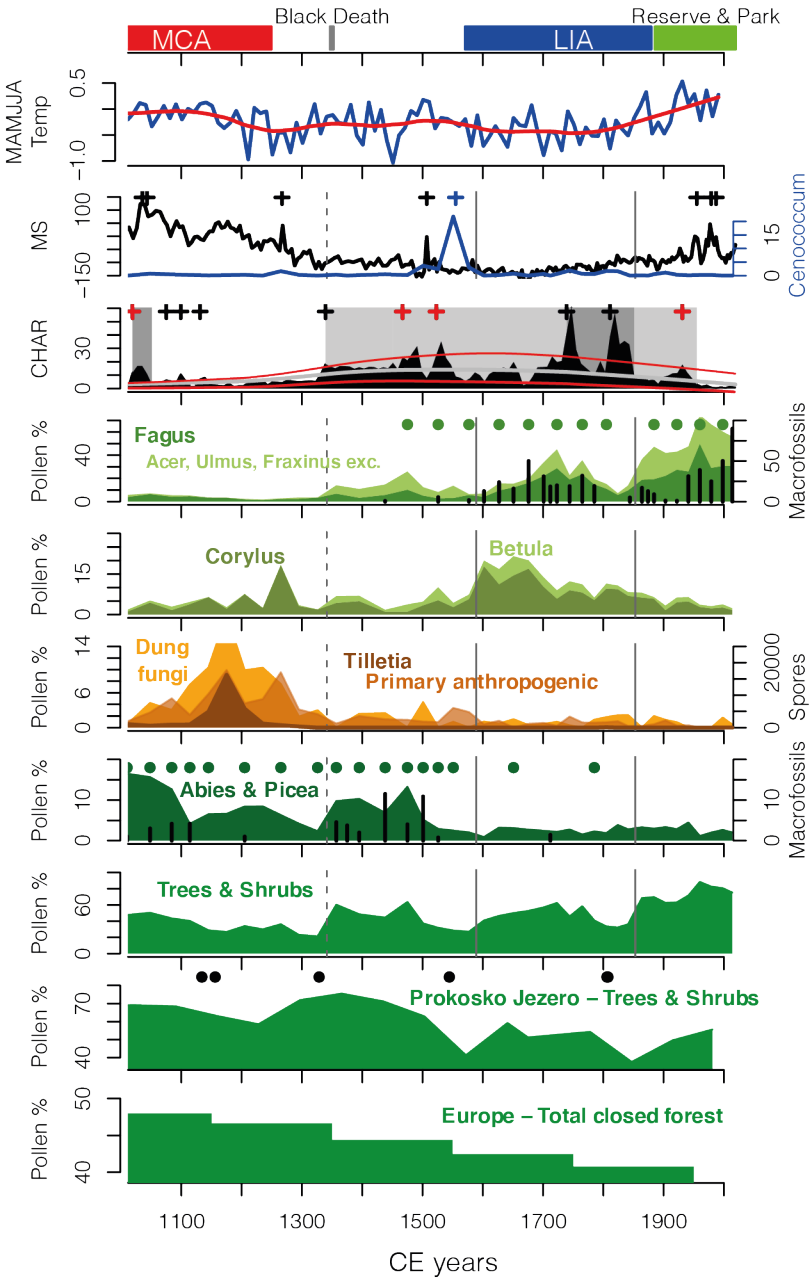
Black Death
MCA
LIA
Reserve & Park
MAMJJA Temp
0.5
−1.0
MS
100
−150
Cenococcum
0
15
CHAR
30
0
Pollen %
Fagus
Acer, Ulmus, Fraxinus exc.
40
0
Macrofossils
50
Corylus
Betula
15
Dung fungi
Tilletia
Primary anthropogenic
14
6
20000
Spores
Abies & Picea
10
Trees & Shrubs
60
Prokosko Jezero – Trees & Shrubs
70
Europe – Total closed forest
1100
1300
1500
1700
1900
CE years

901